

**multi-Risk sciEnce for resilientT commUnities undeR a changiNg  
climate** Codice progetto MUR: **PE00000005** – B73C22001220006



**Deliverable title:** Report on static and dynamic vulnerability models

**Deliverable ID:** DV 3.6.2

**Due date:**31/03/2026

**Submission date:** 31/03/2026

### **AUTHORS**

**Giulio Zuccaro (UNINA), Iunio Iervolino and Georgios Baltzopoulos (UNINA),  
Paolo Castaldo (POLITO), Beatrice Faggiano (UNINA), Fabio Biondini  
(POLIMI), Piero Colajanni and Lidia La Mendola (UNIPA), Sebastiano Foti  
(POLITO), Anna Marzo and Ivan Roselli (ENEA), Gennaro Magliulo (UNINA)**



## 1. Technical references

---

Project Acronym	RETURN
Project Title	multi-Risk sciEnce for resilienT commUnities undeR a changiNg climate
Project Coordinator	Domenico Calcaterra  UNIVERSITA DEGLI STUDI DI NAPOLI FEDERICO II  domcalca@unina.it
Project Duration	December 2022 – November 2025 (36 months)
Deliverable No.	DV3.6.2
Dissemination level*	PU
Work Package	WP3.6. - WP Title: Vulnerability of the built environment: assessment and reduction through sustainable solutions
Task	T3.6.2 - Assessment: static/intrinsic and evolving/dynamic/changing vulnerability
Lead beneficiary	Partner short name
Contributing beneficiary/ies	Partner short name, Partner short name, Partner short name, etc.

\* PU = Public

PP = Restricted to other programme participants (including the Ministry Services)

RE = Restricted to a group specified by the consortium (including the Ministry Services)

CO = Confidential, only for members of the consortium (including the Ministry Services)

## Document history

Version	Date	Lead contributor	Description
0.1	xx.xx.xxxx	First name Last name (Partner short name)	First draft
0.2			Critical review and proofreading
0.3			Edits for approval
1.0			Final version

## 2. ABSTRACT

---

This deliverable presents the research activities carried out within Work Package 3.6 of the RETURN project, focusing on the vulnerability of the built environment and on methods for its assessment and mitigation under multi-hazard conditions and climate change. The work addresses different components of the built environment, including buildings, infrastructure systems and non-structural elements, with the aim of improving the understanding and evaluation of structural vulnerability and resilience.

The first part of the report investigates the evolving vulnerability of the built environment, addressing cumulative damage processes, seismic sequences and ageing effects. Contributions include a framework for cumulative damage assessment in volcanic areas, a Markov-chain-based model for seismic damage accumulation and recovery during earthquake sequences, reliability-based approaches for seismic vulnerability assessment of reinforced concrete structures, and quick-level methodologies for assessing the vulnerability of existing timber buildings considering degradation and durability effects.

The second part focuses on infrastructure vulnerability under multi-hazard and climate change, with particular reference to bridges. Life-cycle approaches are presented to evaluate the effects of environmental degradation, climate change, and fire on the seismic reliability of reinforced concrete bridge piers, as well as advanced numerical frameworks for assessing the seismic performance of bridge foundations affected by scour.

The final part addresses vulnerability assessment of components and facilities, presenting simplified and advanced methods for evaluating the seismic vulnerability of masonry infill walls and methodologies for seismic risk assessment of complex facilities such as hospitals through rapid visual screening and detailed structural analyses.



### 3. Table of contents

---

1. Technical references .....	3
Document history.....	4
2. ABSTRACT .....	5
3. Table of contents.....	7
List of Tables .....	8
List of Figures .....	8
4. Introduction .....	10
4. Evolving vulnerability and resilience of the built environment....	11
4.1 Integrated framework for cumulative damage assessment during pre-eruptive and eruptive phases (UNINA, Giulio Zuccaro) .....	11
4.1.1 Pre-eruptive phase: cumulative seismic damage.....	11
4.1.2 Eruptive phase: volcanic damage and building loss .....	12
4.1.3 Application case: Campi Flegrei cumulative damage simulation .....	12
4.2 Static and dynamic vulnerability models (UNINA, Iunio Iervolino and Georgios Baltzopoulos).....	13
4.2.1 Issues examined .....	13
4.2.2 Methodology.....	14
4.2.3 Illustrative application.....	15
4.2.4 Findings.....	16
4.3 Seismic Vulnerability and Reliability of Structural Systems (POLITO, Paolo Castaldo).....	17
4.3.1 Research activities and objectives .....	17
4.3.2 Conclusions.....	19
4.4 Structural identification tools for a quick level seismic–volcanic vulnerability assessment of existing timber buildings accounting for durability and ageing effects (UNINA, Beatrice Faggiano) .....	19
The survey forms for existing timber structures .....	19
Mechanical characterization of existing timber structures through non destructive tests	21
Conclusion:.....	23
5. Infrastructure vulnerability under multi-hazard and climate change .....	24
5.1 Life-cycle seismic vulnerability of bridges under climate change (POLIMI, Fabio Biondini)	24
5.1.1 Life-cycle seismic performance of bridges .....	24
5.1.2 Effects of Climate Change.....	24
5.1.3 Case Study.....	25
5.1.4 Conclusions.....	26

5.2 Assessment of multi-risk vulnerability for existing bridges (aging, fire, earthquake) (UNIPA, Piero Colajanni and Lidia La Mendola).....	26
5.2.1 Bridges vulnerability to seismic action, aging and fire.....	26
5.2.2 Methodology.....	26
5.2.3 Results of parametric analyses and Case Study.....	27
5.3 Development and validation of innovative techniques for integrated rehabilitation – Residual seismic capacity of bridges across rivers (POLITO, Sebastiano Foti).....	28
5.2.1 Context and Problem Statement.....	28
5.2.2 Experimental Characterization of SoFSI Sand.....	28
5.2.3 Constitutive Modeling and Numerical Implementation.....	28
5.2.4 Performance Analysis and Seismic Findings.....	29
5.2.5 Conclusions.....	29
<b>6. Vulnerability assessment methods for non-structural components and facilities.....</b>	<b>30</b>
6.1 Method to assess the frame-infill interaction in combined structural and energetic solutions (ENEA, Anna Marzo and Ivan Rosselli).....	30
6.1.1 Infill panel FEM models and analyses.....	30
6.1.2 Conclusions.....	32
6.2 Seismic Risk Assessment Methodologies (UNINA, Gennaro Magliulo).....	32
<b>5. Conclusions.....</b>	<b>35</b>
<b>6. References.....</b>	<b>36</b>

## List of Tables

**Table 1:** Unit-time recovery matrix

**Table 2:** Outline of the SHA-T survey form

**Table 3:** Outline of the IIWC survey form

## List of Figures

**Figure 1:** Distribution of buildings among vulnerability classes resulting from the iterative application of the cumulative damage procedure over the sequence of eight consecutive seismic events in the Phlegraean Area, based on two alternative seismic hazard representations: (a) INGV shakemaps; (b) shakemaps derived using Scala et al Law (b)

**Figure 2:** Sketch of the phenomenon, which is the target of the question (adopted from Cox and Miller 1965)

**Figure 3:** CCDF at the site of L'Aquila assuming that a M6.3 mainshock occurred

**Figure 4:** Damage probabilities over time with and without recovery

**Figure 5:** Seismic fragility curves - safety limit state-LS3 of the maximum interstorey drift index: (a) code seismic design, (b) proposed seismic design

**Figure 6:** Schematization of fibre beam-column element (a) with the bar buckling and bar slip model (b); Comparison between the different approaches for evaluating the probability (c)

**Figure 7:** Failure probabilities considering confined concrete (a); cyclic design process (b)

**Figure 8:** Main sections of the SHA-T survey form, applied to Palazzo Petrucci (Naples) (Faggiano et al., 2022)

**Figure 9:** Case studies for the application of the SHA-T survey form (Marranzini et al., 2023)

**Figure 10:** Example of application of the IWC form to the Royal Palace of Naples (Faggiano et al., 2025)

**Figure 11:** Specimen and Methods (Verre et al., 2023; Marranzini et al., 2025)

**Figure 12:** Some of the linear correlations analyzed (Marranzini et al., 2025)

**Figure 13:** Life-cycle seismic reliability assessment of a RC bridge pier under historical and climate change scenarios: (a) Geometry; (b) Nominal base-shear versus pier drift; (c) Time-variant reliability index

**Figure 14:** Fragility curves for RC bridge circular piers under seismic, aging and fire scenarios: (a) geometry; (b) longitudinal direction; (c) transversal direction (d)

**Figure 15:** (A-C) DSS tests: A) specimen assembled in the DSS device; B-C) Results of DSS tests at a normal effective stress of 50 kPa, in terms of shear stress (B) and void ratio (C) vs shear strain loops. (D-E) Numerical model: D) Sketch of the numerical model, in the LS scenario, E) influence of the scour scenario on the deck spectral acceleration, for varying free-field spectral amplitude

**Figure 16:** a) Method for preliminary estimation of infill wall vulnerability. b) Explanatory example

**Figure 17:** Numerical tests on: a) mortar specimen; b) hollow clay brick; c) fully restrained infill wall

**Figure 18:** Example of failure probability curves in case of panels having: a) restrained edges; b) gap at upper edge; c) gap at side edges

## 4. Introduction

---

Assessing and reducing the vulnerability of the built environment is a central objective for improving the resilience of communities exposed to natural hazards. In many regions, particularly in countries characterized by complex hazard scenarios such as Italy, the built environment is exposed to multiple threats including earthquakes, volcanic phenomena, environmental degradation and climate-related hazards. These factors may interact over time and progressively reduce the structural capacity of buildings and infrastructure systems, increasing the risk for communities and critical facilities.

Within the RETURN project, Work Package 3.6 addresses the vulnerability of the built environment and the development of innovative approaches for its assessment and reduction through sustainable solutions. In this context, the present deliverable collects the contributions developed by several research units, focusing on different aspects of structural vulnerability and resilience.

The first part of the deliverable examines the temporal evolution of vulnerability and resilience in the built environment, considering cumulative damage processes and degradation phenomena. Approaches are presented to model the accumulation of damage during seismic sequences, evaluate the reliability of structural systems under repeated events and ageing effects, and develop rapid methodologies for assessing the vulnerability of existing timber structures exposed to seismic and volcanic hazards.

The second part addresses the vulnerability of infrastructure systems under multi-hazard conditions (aging, corrosion, fire) and climate change, with particular attention to bridge structures. The studies presented analyze the effects of environmental deterioration processes, such as corrosion, and the interaction between seismic loading and foundation degradation caused by scour.

The final part focuses on vulnerability assessment at the component and facility scale, highlighting the importance of non-structural elements and operational aspects in determining the overall seismic risk of buildings and strategic facilities. Methods are proposed for evaluating the vulnerability of masonry infill walls and for assessing seismic risk in complex facilities such as hospitals through rapid visual screening and advanced structural analyses.

Together, these contributions provide complementary perspectives and methodologies aimed at improving the understanding, assessment and management of vulnerability in the built environment under evolving hazard conditions.

## 4. Evolving vulnerability and resilience of the built environment

---

The vulnerability of the built environment evolves over time due to cumulative damage, degradation processes and the interaction between multiple hazards. This section presents approaches aimed at modelling the temporal evolution of structural vulnerability and the mechanisms influencing resilience. An integrated framework for cumulative damage assessment in volcanic areas is introduced, in which repeated seismic events progressively reduce structural capacity during the pre-eruptive phase, while volcanic hazards may lead to building loss. The framework is applied to the Campi Flegrei area to simulate the evolution of vulnerability under recent seismic activity. Complementary studies address the modelling of seismic damage accumulation and recovery during earthquake sequences through a Markov-chain-based approach, as well as the assessment of seismic vulnerability and reliability of reinforced concrete structural systems under cumulative seismic actions. Finally, a quick-level methodology for the vulnerability assessment of existing timber buildings is proposed, integrating durability, ageing effects and in-situ mechanical characterization through non-destructive testing techniques.

### 4.1 Integrated framework for cumulative damage assessment during pre-eruptive and eruptive phases (UNINA, Giulio Zuccaro)

The assessment of damage to buildings in volcanic areas requires consideration of the temporal evolution of different hazard processes and their cumulative effects [1]. Damage mechanisms developing during the pre-eruptive phase differ substantially from those characterizing the eruptive phase in terms of underlying physical processes, structural response, and applicable assessment scales. For this reason, the proposed framework adopts a phase-dependent modeling strategy, ensuring internal consistency maintaining a clear and coherent interpretation of results.

#### 4.1.1 Pre-eruptive phase: cumulative seismic damage

During the pre-eruptive phase, seismic activity typically represents the dominant hazard. Damage accumulation is driven by repeated seismic events and is modeled as a progressive reduction of structural capacity.

Under initial (peace-time) conditions, the building stock is distributed among four seismic vulnerability classes (A–D), where A denotes the most vulnerable buildings and D the least vulnerable one. Following each seismic event, structural damage is estimated according to the European Macroseismic Scale (EMS-98), which defines six damage grades (D0–D5), ranging from no damage (D0) to total collapse (D5).

Seismic damage is not treated as an isolated outcome of a single event, but as a permanent reduction of structural capacity. This reduction is modeled through transitions between vulnerability classes, providing a synthetic representation of cumulative structural weakening. Two additional high-vulnerability classes (AA and AAA) are introduced to represent severely compromised but still standing buildings.

The updating rules after each seismic event are as follows:

- Buildings with D4–D5 damage (partial or total collapse) are considered permanently lost and removed from the stock.
- Buildings with D3 damage (severe structural damage) are shifted by two vulnerability classes.
- Buildings with D2 damage (slight structural damage) are shifted by one vulnerability class.
- Buildings with D0–D1 damage retain their original class.

Through iterative application of these rules, the distribution of buildings among vulnerability classes is updated after each event, explicitly incorporating pre-existing damage. The updated distribution

represents the current structural condition of the building stock and forms the basis for subsequent assessments within the pre-eruptive phase.

#### 4.1.2 Eruptive phase: volcanic damage and building loss

During the eruptive phase, additional volcanic hazards such as ash fall and pyroclastic density currents may affect the built environment. The associated damage mechanisms differ significantly from seismic loading and cannot be appropriately described using seismic damage scales.

For this reason, volcanic damage is modeled through a binary classification: buildings are either lost or not lost. No transitions between vulnerability classes are introduced during this phase. Buildings classified as lost due to volcanic phenomena are removed from the stock, while undamaged buildings retain the vulnerability class reached at the end of the pre-eruptive phase.

This modeling choice preserves a clear conceptual distinction between cumulative seismic degradation and volcanic-induced building loss, avoiding the inappropriate extension of seismic damage metrics to non-seismic phenomena.

#### 4.1.3 Application case: Campi Flegrei cumulative damage simulation

The proposed procedure was applied to the Campi Flegrei area to simulate the cumulative evolution of damage resulting from recent seismic activity.

The initial distribution of buildings among vulnerability classes was derived according to the methodology described in Deliverable D3.6.1. Although data collection occurred after the first seismic events, pre-existing structural damage was not explicitly considered; therefore, the vulnerability classification was assumed representative of peace-time conditions and adopted as the initial simulation state

All seismic events with magnitude greater than 4 occurring in the Campi Flegrei area from 2023 to the present were considered, resulting in a chronological sequence of eight events. These were used to iteratively simulate damage accumulation during the pre-eruptive phase. To investigate the influence of hazard representation, two alternative seismic processing approaches were adopted: (a) the use of INGV peak ground acceleration (PGA) maps converted into macroseismic intensity through the Margottini law; (b) the application of Scala et al [2] procedure, specifically calibrated for volcanic-type earthquakes and consistent with Campi Flegrei seismicity.

For both approaches, the sequence of eight events was applied iteratively to update the building stock according to the cumulative damage rules. The results allow for a comparison of the temporal evolution of vulnerability class distribution and cumulative building losses under different seismic hazard representations.

Figure 1 presents the vulnerability class redistribution resulting from the iterative application of the damage updating procedure under two alternative seismic hazard representations, emphasizing the sensitivity of exposure evolution to the adopted shakemap model. The diagrams show a progressive concentration of buildings in higher vulnerability classes as cumulative damage develops over the seismic sequence. Although both hazard representations produce a consistent qualitative trend, differences emerge in the magnitude of redistribution and associated building losses. This confirms the sensitivity of cumulative damage assessment to the adopted seismic input model.

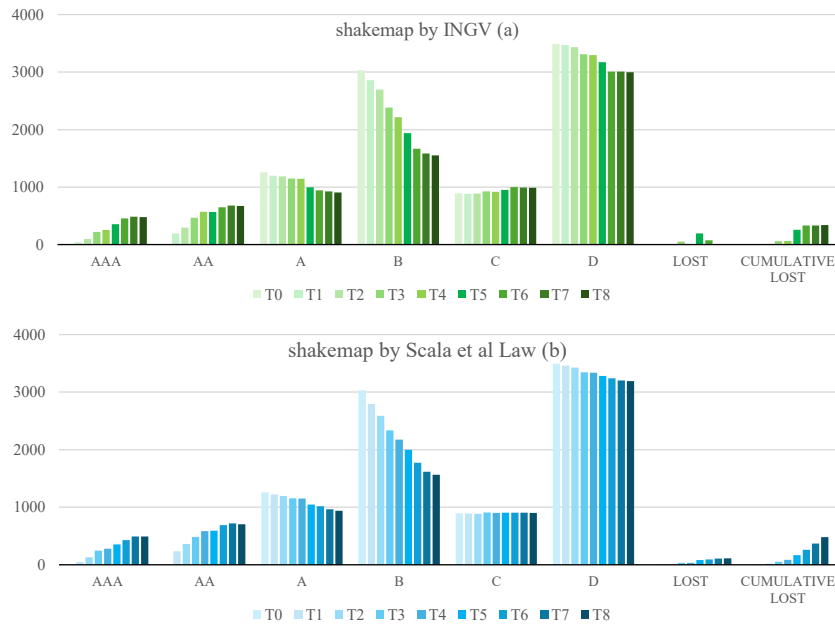


Figure 1: Distribution of buildings among vulnerability classes resulting from the iterative application of the cumulative damage procedure over the sequence of eight consecutive seismic events in the Phlegraean Area, based on two alternative seismic hazard representations: (a) INGV shakemaps; (b) shakemaps derived using Scala et al Law (b)

## 4.2 Static and dynamic vulnerability models (UNINA, Iunio Iervolino and Georgios Baltzopoulos)

Earthquakes typically occur in time-space clusters. Classical probabilistic seismic risk analysis, only consider the prominent magnitude earthquakes within each cluster. This implicitly corresponds to neglect that, for exposed infrastructure, the clustering behaviour of seismic events may, on one hand, cause damage accumulation and prolonged business interruption and, on the other hand, may delay or disrupt the repair and recovery processes. In the deliverable, a Markov-chain-based model, able to describe both loss and recovery during aftershock sequences is presented. It preserves most of the benefits of the classical approach and can be extended to enable modelling of peculiar resilience features such as delay in recovery initiation.

### 4.2.1 Issues examined

Earthquake clusters are made of the mainshock and its contouring events, foreshocks and aftershocks, respectively. Stochastic modelling of seismic clusters' occurrence, and related shaking at a site of interest, can consist in a hierarchical approach in which mainshocks' occurrence follows a homogeneous Poisson process, whereas the other seismic events in each cluster follow a conditional process (Iervolino et al. 2014). For example, aftershock occurrence can be modelled as a non-homogeneous Poisson process, the intensity of which depends on some mainshock features (Yeo and Cornell 2009). In the context of seismic risk analysis this can be referred to as hazard modelling.

Any system of interest exposed to seismic risk is virtually vulnerable to each event of a cluster, and seismic loss can accumulate in multiple partially damaging events. This is especially true in the most hazardous part of the cluster, which is around the mainshock, because of the short interarrival time between earthquakes. This issue can be treated as a form of stochastic degradation process, and Markov processes (i.e., Markov chains) have been shown being suitable to describe it (Iervolino et al. 2016, Iervolino et al. 2020). This approach to model seismic vulnerability makes use of the system's state-dependent fragility functions.

Repair is one of the possible strategies to recover from seismic loss. Recovery modelling is necessary for the resilience assessment (Bruneau et al. 2003). Research shows that the starting of the repair process can be delayed by factors such as the availability of resources and administrative issues (Costa et al. 2020). As mentioned above, also the time-space concentration of seismic events can temporarily delay or disrupt the recovery (Iervolino and Giorgio 2015).

The research question is about developing a holistic Markovian model that enables a holistic modelling of seismic damage (yet neglecting foreshocks) for a system of interest. This was first envisaged in (Chioccarelli et al. 2021) and is conceptually formulated herein. Figure 2 sketches the phenomenon which is the subject of the modelling question.

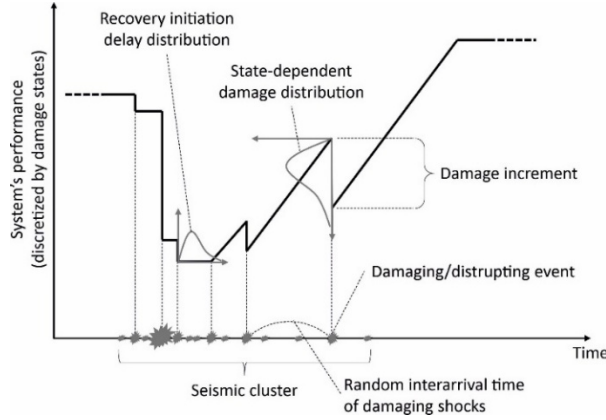


Figure 2: Sketch of the phenomenon, which is the target of the question (adopted from Cox and Miller 1965)

#### 4.2.2 Methodology

Aftershock probabilistic seismic hazard analysis (APSHA; Yeo and Cornell 2009) models the occurrence of aftershock according to a non-homogeneous Poisson process; i.e., characterized by a time-variant rate. In this context, the evolution over time of the seismic damage accumulation and recovery in aftershock sequences can be described by using a non-homogeneous Markov chain, where both the damage level and the time elapsed from the mainshock are measured on discrete scales. Given the probability vector of the initial state, the model is fully defined by its transition matrix. This matrix, indicated as  $[P(k, k + 1)]$ , contains the probabilities that in each time unit the system passes from a given damage state to another, as:

$$[P(k, k + 1)] = \begin{bmatrix} p_{1,1}(k) & p_{1,2}(k) & p_{1,3}(k) & p_{1,4}(k) \\ p_{2,1}(k) & p_{2,2}(k) & p_{2,3}(k) & p_{2,4}(k) \\ p_{3,1}(k) & p_{3,2}(k) & p_{3,3}(k) & p_{3,4}(k) \\ p_{4,1}(k) & p_{4,2}(k) & p_{4,3}(k) & p_{4,4}(k) \end{bmatrix}. \quad (1)$$

The size of the transition matrix refers to the chosen partition of the system's quality (i.e., performance) function; in the example, four damage states (i.e.,  $DS_1, \dots, DS_4$ ), ordered by increasing severity, are considered. The parameter  $k$  indicates the number of units of time elapsed from the mainshock. The generic element,  $p_{i,j}(k)$ , represents the conditional probability that the system, which is in state  $D(k) = DS_i$  at time  $k$ , is in  $D(k + 1) = DS_j$  at time  $k + 1$ , that is:

$$p_{i,j}(k) = P[D(k + 1) = DS_j | D(k) = DS_i]. \quad (2)$$

The transition matrix can be formulated as:

$$[P(k, k + 1)] = v(k) \cdot [D] + [1 - v(k)] \cdot [R] = v(k) \cdot \begin{bmatrix} d_{1,1} & d_{1,2} & d_{1,3} & d_{1,4} \\ 0 & d_{2,2} & d_{2,3} & d_{2,3} \\ 0 & 0 & d_{3,3} & d_{3,4} \\ 0 & 0 & 0 & 1 \end{bmatrix} + [1 - v(k)] \cdot \begin{bmatrix} 1 & 0 & 0 & 0 \\ r_{2,1} & r_{2,2} & 0 & 0 \\ r_{3,1} & r_{3,2} & r_{3,3} & 0 \\ r_{4,1} & r_{4,2} & r_{4,3} & r_{4,4} \end{bmatrix}, \quad (3)$$

where  $v(k)$  is the rate of aftershock occurrence evaluated at time  $k$  (which is dependent on the magnitude of the mainshock).  $D$  is the matrix that contains the (conditional) probabilities of transitions determined by a generic aftershock (of unspecified magnitude and location), that is those of the type  $DS_i \rightarrow DS_j$ ,  $i \leq j$ .  $R$  is the matrix that contains the (conditional) probabilities of transitions of the type  $DS_i \rightarrow DS_j$ ,  $i \geq j$ , because of the recovery activities. The model assumes that in a unit of time only one of these two types of transitions can occur. For the model to work, it should be  $v(k) \ll 1$ , that is achieved by assuming a time scale in which units are small enough.

The probability vector of the state of the system at time  $m$ ,  $P(m) = [P_1(m), \dots, P_4(m)]$ , where  $P_l(m) = P[D(m) = DS_l]$ ,  $l = 1, \dots, 4$ , can be obtained as:

$$P(m) = P(0) \cdot \prod_{k=0}^{m-1} [P(k, k + 1)]. \quad (4)$$

The probability vector of the initial state  $(0) = [P_1(0), \dots, P_4(0)]$ , refers to the damage state of the system immediately after the mainshock.

Apparently, the model in equation (3) cannot describe the early phase of the recovery process that usually shows a delay in starting the recovery activities (i.e., Figure 2). In fact, a more general Markovian model (i.e., a Markov chain), which can also address this issue, can be formulated by using the device of stages (DOS) technique (e.g., Iervolino et al. 2020). DOS entails modeling a non-exponential sojourn time by a proper arrangement of stages in which sojourn time is exponentially distributed, enabling to deal non-Markovian processes via the Markovian theory.

### 4.2.3 Illustrative application

An illustrative example of the described framework is reported here. The structure considered is a six-story, code-conforming reinforced concrete frame building, supposedly located at the site of L'Aquila, Italy. Five damage states are considered to describe the increasing structural damages (i.e.,  $DS_1, \dots, DS_5$ ). The corresponding state-dependent fragility functions are those developed in (Orlacchio et al. 2024); they refer to the spectral acceleration (Sa) at vibration period equal to 0.5 s,  $Sa(0.5s)$ , and provide, via a lognormal model, the probability of exceeding a damage state,  $DS_j$ , conditional on the intensity measure and the damage state in which the earthquake finds the structure,  $DS_i$ , according to the following equation:

$$P[DS \geq DS_j | DS_i, Sa(0.5s) = sa] = \Phi \left( \frac{\ln(sa) - \ln(\bar{sa}^{i,j})}{\sigma_{\ln \bar{sa}^{i,j}}} \right). \quad (5)$$

In the equation  $\ln(\bar{sa}^{i,j})$  and  $\sigma_{\ln \bar{sa}^{i,j}}$  are the median and the logarithmic standard deviation of the intensity measure, respectively, and they define the model.

The unit time transition probability matrix is obtained by integrating the state dependent fragility functions with the probability density function derived by the complementary cumulative distribution function, conditional on the occurrence of one generic aftershocks, as reported in Figure 3. It results from an aftershock probabilistic seismic hazard analysis (APSHA, Iervolino et al. 2014) performed for the site of L'Aquila, assuming that an M6.3 mainshock has occurred.

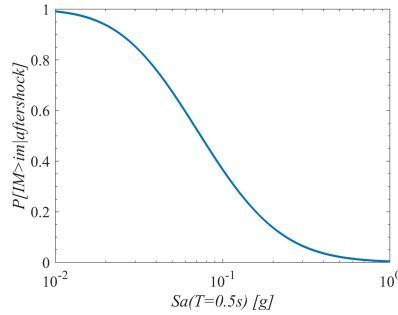


Figure 3: CCDF at the site of L'Aquila assuming that a M6.3 mainshock occurred

The unit time (i.e., six months) recovery matrix is assumed as reported in Table 1:

Table 2 - Unit-time recovery matrix

	$DS_1$	$DS_2$	$DS_3$	$DS_4$	$DS_5$
$DS_1$	1	0	0	0	0
$DS_2$	0.4	0.6	0	0	0
$DS_3$	0.4	0	0.6	0	0
$DS_4$	0	0	0.2	0.8	0
$DS_5$	0	0	0	0.2	0.8

The probability of finding the structure in  $DS_1$ , given that it was damaged to  $DS_3$  by the mainshock, is reported in Figure 4a, considering or neglecting the recovery component of the model. In the first case, that is, with recovery, the probability monotonically increases with the time since the mainshock. As expected, this probability is constant and equal to zero when no recovery strategy is assumed. Figure 4b shows the probability of  $DS_5$  for the same structure, which is assumed to be in  $DS_3$  after the mainshock. If no recovery is considered, the probability slightly increases after the mainshocks and, because the rate of aftershocks reduces with time, becomes constant. On the other hand, when the recovery matrix is considered, after some time since the mainshock, the rate of aftershocks becomes negligible and the probability of a worsened condition decreases.

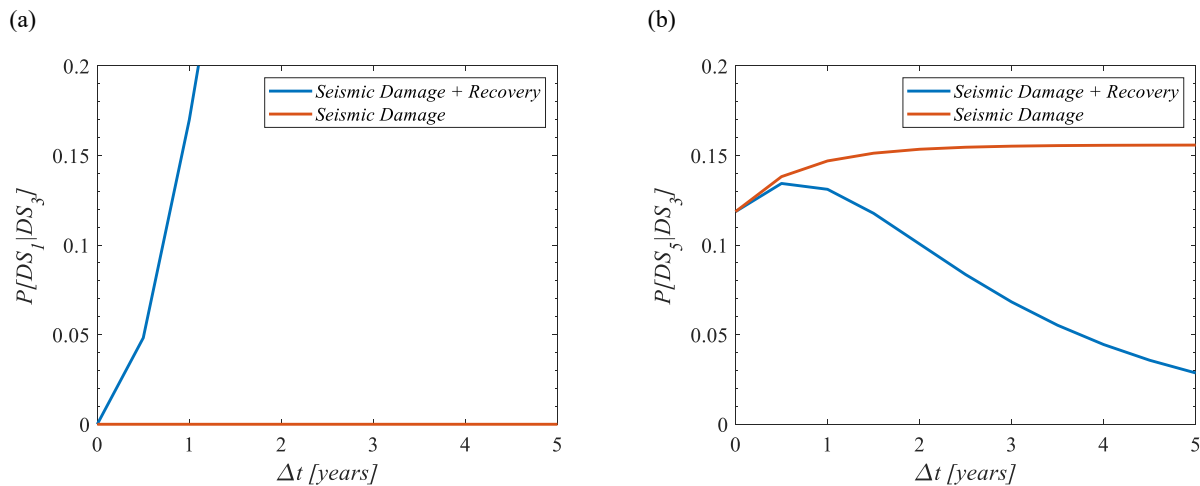


Figure 4: Damage probabilities over time with and without recovery

#### 4.2.4 Findings

Building on previous works on the topic by the authors, a holistic Markovian model for seismic damage accumulation and recovery during seismic sequences was formulated. The model works in the hypothesis of aftershock probabilistic seismic hazard analysis, that is, following a mainshock of known features. Its

main limitations are: (i) that it neglects foreshocks, and (ii) that it does not explicitly model the typical random delay in starting the recovery activities. However, both these issues can be addressed by suitable adjustments of the model. For example, issue (ii) can be readily solved by using the DOS technique.

## 4.3 Seismic Vulnerability and Reliability of Structural Systems (POLITO, Paolo Castaldo)

The POLITO-CASTALDO research unit has developed models for vulnerability assessment of the built environment accounting for aging and degradation processes and models for the assessment of seismic vulnerability as a function of the cumulative damage induced by sequences of seismic events combined with other external actions. In addition, a reliability-based methodology for the seismic retrofitting design of non-ductile reinforced concrete frame structures for different return periods, and the influence on seismic vulnerability of confinement effects in concrete affecting the capacity design principles have been investigated. In addition, new proposals in terms of control algorithms to improve the seismic performance of asymmetric buildings equipped with viscous devices are presented.

The research unit also elaborated the results from numerical analyses to assess the seismic vulnerability, reliability and robustness of reinforced concrete systems with respect to different events. At the same time, new methodologies have been proposed to assess structural safety to any external action by means of non-linear global analysis to different external actions considering both the aleatory and epistemic uncertainties.

Finally, the research unit implemented different machine learning models to predict the seismic performance of structural systems with respect to specific characteristics of the ground motions.

### 4.3.1 Research activities and objectives

An objective has been to improve the design methodology by including explicitly the confinement effects within the seismic design of a new RC frame due to their influence on the capacity design principles. Moreover, a comparison between three constitutive models (i.e., Model 1, Model 2, Model 3) for confined concrete is performed (Figure 5). More details may be found in (Miceli et al., 2024).

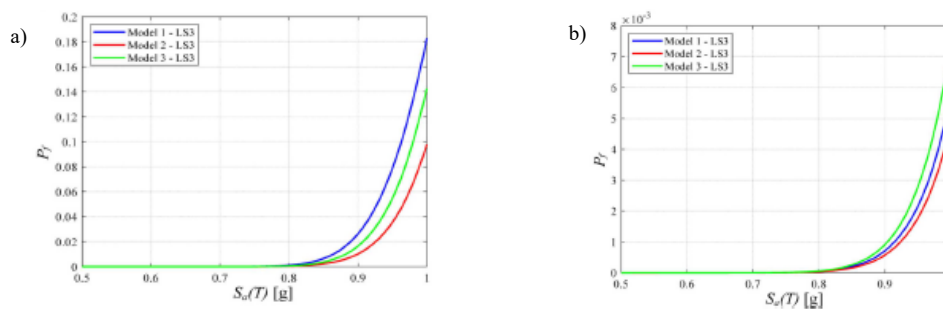


Figure 5: Seismic fragility curves - safety limit state-LS3 of the maximum interstory drift index: (a) code seismic design, (b) proposed seismic design

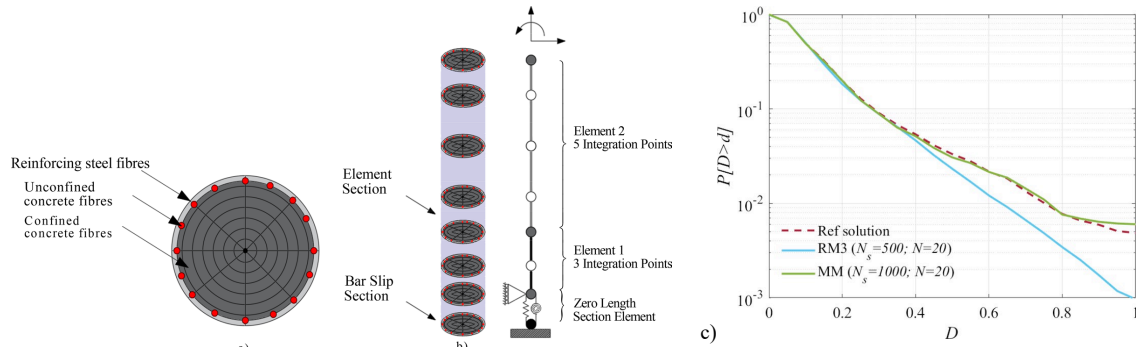


Figure 6: Schematization of fibre beam-column element (a) with the bar buckling and bar slip model (b); Comparison between the different approaches for evaluating the probability (c)

A regression-based model (RBM) and a Markov-chain based Method (MM) are compared including some improvements. The comparison between the methodologies is carried out by examining a reinforced concrete (RC) bridge pier model (Figure 6) and using the Park-Ang damage index ( $D$ ) to describe the damage accumulation. The expected results include the determination of the probability of excess seismic demand as a function of the number of secondary events as shown in Figure 6(c) (denoted as RM3, for a number of earthquake sequences  $N_s = 500$  and a total number of shocks  $N = 20$ ) and of the MM (for  $N_s = 1000$  and  $N = 20$ ). More details may be found in (Turchetti et al., 2023).

In addition, a comprehensive, reliability-based methodology for the seismic retrofitting design of non-ductile RC frame structures is proposed. It advances the innovative application of the Performance-Based Earthquake Engineering framework to the retrofitting of non-code-compliant buildings. The proposal offers a cost-effective strategy that balances seismic performance, quantified in terms of the Mean Return Period of limit state exceedances, with retrofit costs. More details may be found in (Sberna et al., 2025).

Moreover, new strategies for the semi-active control of the dynamic response of a plan-wise asymmetrical structural system using viscoelastic devices have been proposed. These innovative strategies are designed to optimize the different terms of the energy balance equation through a set of closed-form analytical control algorithms to manage the properties of semi-active devices. Specifically, four algorithms have been developed to maximize the energy dissipated by the system or minimize the elastic energy, kinetic energy, and input energy. More details may be found in (De Iuliis et al., 2025).

Successively, the research unit examined the numerical results to assess the seismic vulnerability, reliability and robustness of RC systems with respect to different events. Specifically, a 5-storey and 4-span 2D RC moment resisting frame is considered, designed in a highly seismic area according to both Italian and European codes. Subsequently, through a cyclic design procedure (Figure 7), some modifications are suggested regarding the layout of the longitudinal reinforcement bars. It has also been proposed to assess the robustness assessment of 3D RC structures by means of the superposition of the response of the 2D frames in different design configurations and failure scenarios. More details may be found in (Miceli and Castaldo, 2024, Miceli et al., 2023, Miceli et al., 2025, Miceli et al., 2025).

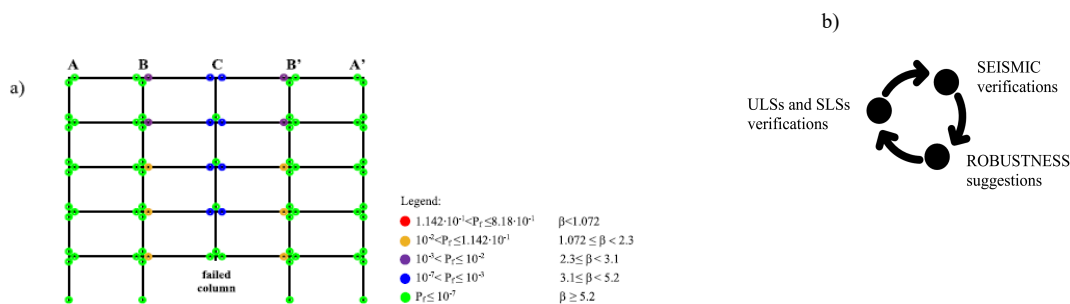


Figure 7: Failure probabilities considering confined concrete (a); cyclic design process (b)

Finally, the research unit also implemented different machine learning (ML) models to predict the seismic response of systems with respect to specific characteristics of the ground motions. In this way, the high predictive seismic parameters set, characterizing ground motions, has been defined. To validate the results obtained, the most effective model predictions have been compared with the results of the

parametric step-by-step analyses. Additionally, a further investigation has been finalized using appropriate indices within Information Theory. More details may be found in (De Iuliis et al., 2024, De Iuliis et al., 2025).

### 4.3.2 Conclusions

The research unit examined the seismic vulnerability to main earthquakes or sequences of earthquakes on structural systems. The results highlight the computational efficiency and accuracy of the proposed approach, validating its utility in real-world scenarios.

As for structural robustness, the results confirm that the continuity of the longitudinal rebars as well as the side face rebars are two crucial design improvements to achieve a design able to respect the principles of both earthquake engineering and robustness.

As for ML models, the research unit also implemented different ML models effective to predict the seismic performance of structural systems with respect to specific characteristics of the ground motions investigating the information of specific seismic parameters characterising the input records.

## 4.4 Structural identification tools for a quick level seismic–volcanic vulnerability assessment of existing timber buildings accounting for durability and ageing effects (UNINA, Beatrice Faggiano)

The research activity deals with the development of a quick-level methodology for the structural vulnerability assessment of existing timber buildings exposed to seismic and volcanic hazards, also explicitly incorporating durability and ageing effects into the evaluation process. In particular, to support the methodology, two survey tools were developed and applied to case studies, the SHA-T form, for guiding data collection from the building identification to the decay diagnosis, and the IIWC form, specially tailored for the survey of heritage timber truss structural systems. It is noticeable that in order to identify the structural capabilities of existing timber constructions, in situ mechanical characterization through non-destructive testing (NDT) is required, as it provides information on the state of conservation and residual strength and stiffness of the load-bearing elements without compromising the integrity. With this regards, a contribution is given to the definition and evaluation of statistical correlations between the non-destructive and destructive tests (DT) measures on ancient timber elements, with the aim of calibrating and validating the reliability of in situ techniques against the actual mechanical properties of the material.

### The survey forms for existing timber structures

The research activity focuses on developing a quick-level approach for the structural vulnerability assessment of the existing timber structures exposed to seismic and volcanic risks, taking into account durability and ageing issues (Marranzini et al., 2023). The approach is based on the combined application of semi-quantitative methods for the estimation of seismic-volcanic vulnerabilities and state of conservation, with the final goal of developing a methodology that enables the vulnerability assessment through the definition of an integrated vulnerability index. The acquisition of reliable data, the quality and completeness of the collected information on existing buildings appear to be a fundamental step. To this aim, two ad hoc survey forms have been developed for the acquisition of data on vulnerability criteria and durability aspects. The first one, inspired by the DPC-Reluis CARTIS form (Zuccaro et al., 2015), is a survey form for the Structural Health Assessment (SHA) of the existing Timber (T) structures (Faggiano et al., 2022; Marranzini et al., 2023), as an operational tool guiding descriptive procedure, which could be used even by not expert technicians. The form is conceived through a top-down approach, going from the localization of the building to the diagnosis of the degradation phenomena. The SHA-T form consists of the following 3 macro-sections: *building identification*; *timber decay detection*; *interventions and treatments* (Fig.8; Tab. 2).

<p><b>Section B: Identification of the building constructive technology and typology</b></p> <p><b>B1) Material classification</b></p> <table border="1"> <thead> <tr> <th>Materials</th> <th>Vertical</th> <th>Intermediate floors</th> <th>Roof</th> <th>Foundation</th> </tr> </thead> <tbody> <tr><td>R.C.</td><td><input type="checkbox"/></td><td><input type="checkbox"/></td><td><input type="checkbox"/></td><td><input type="checkbox"/></td></tr> <tr><td>Prefabricated R.C.</td><td><input type="checkbox"/></td><td><input type="checkbox"/></td><td><input type="checkbox"/></td><td><input type="checkbox"/></td></tr> <tr><td>Steel</td><td><input type="checkbox"/></td><td><input type="checkbox"/></td><td><input type="checkbox"/></td><td><input type="checkbox"/></td></tr> <tr><td>Timber</td><td><input type="checkbox"/></td><td><input type="checkbox"/></td><td><input type="checkbox"/></td><td><input type="checkbox"/></td></tr> <tr><td>Masonry</td><td><input type="checkbox"/></td><td><input type="checkbox"/></td><td><input type="checkbox"/></td><td><input type="checkbox"/></td></tr> <tr><td>Composite Steel-RC</td><td><input type="checkbox"/></td><td><input type="checkbox"/></td><td><input type="checkbox"/></td><td><input type="checkbox"/></td></tr> <tr><td>Absent</td><td><input type="checkbox"/></td><td><input type="checkbox"/></td><td><input type="checkbox"/></td><td><input type="checkbox"/></td></tr> <tr><td>Not identified</td><td><input type="checkbox"/></td><td><input type="checkbox"/></td><td><input type="checkbox"/></td><td><input type="checkbox"/></td></tr> <tr><td>Other materials</td><td><input type="checkbox"/></td><td><input type="checkbox"/></td><td><input type="checkbox"/></td><td><input type="checkbox"/></td></tr> </tbody> </table> <p><b>B2) Structural typology and relation with floors</b></p> <table border="1"> <thead> <tr> <th>Vertical structure</th> <th>Absent</th> <th colspan="3">Seismic resistant system</th> </tr> <tr> <th>Intermediate floor</th> <th></th> <th>Frame</th> <th>Walls</th> <th>Archs</th> </tr> </thead> <tbody> <tr><td>Absent</td><td><input type="checkbox"/></td><td><input type="checkbox"/></td><td><input type="checkbox"/></td><td><input type="checkbox"/></td></tr> <tr><td>Not identified</td><td><input type="checkbox"/></td><td><input type="checkbox"/></td><td><input type="checkbox"/></td><td><input type="checkbox"/></td></tr> <tr><td>In plane deformable floor</td><td><input type="checkbox"/></td><td><input type="checkbox"/></td><td><input type="checkbox"/></td><td><input type="checkbox"/></td></tr> <tr><td>In plane rigid floor</td><td><input type="checkbox"/></td><td><input type="checkbox"/></td><td><input type="checkbox"/></td><td><input type="checkbox"/></td></tr> </tbody> </table> <p><b>B3) Bracing system</b></p> <table border="1"> <thead> <tr> <th rowspan="2">Materials</th> <th colspan="2">Transv. Dir.</th> <th colspan="2">Long. Dir.</th> </tr> <tr> <th>Timber</th> <th>Steel</th> <th></th> <th></th> </tr> </thead> <tbody> <tr><td>Single diagonal</td><td><input type="checkbox"/></td><td><input type="checkbox"/></td><td><input type="checkbox"/></td><td><input type="checkbox"/></td></tr> <tr><td>MRF</td><td><input type="checkbox"/></td><td><input type="checkbox"/></td><td><input type="checkbox"/></td><td><input type="checkbox"/></td></tr> <tr><td>Concentric X braces</td><td><input type="checkbox"/></td><td><input type="checkbox"/></td><td><input type="checkbox"/></td><td><input type="checkbox"/></td></tr> <tr><td>Concentric K braces</td><td><input type="checkbox"/></td><td><input type="checkbox"/></td><td><input type="checkbox"/></td><td><input type="checkbox"/></td></tr> <tr><td>Concentric V braces</td><td><input type="checkbox"/></td><td><input type="checkbox"/></td><td><input type="checkbox"/></td><td><input type="checkbox"/></td></tr> <tr><td>Eccentric braces</td><td><input type="checkbox"/></td><td><input type="checkbox"/></td><td><input type="checkbox"/></td><td><input type="checkbox"/></td></tr> </tbody> </table>	Materials	Vertical	Intermediate floors	Roof	Foundation	R.C.	<input type="checkbox"/>	<input type="checkbox"/>	<input type="checkbox"/>	<input type="checkbox"/>	Prefabricated R.C.	<input type="checkbox"/>	<input type="checkbox"/>	<input type="checkbox"/>	<input type="checkbox"/>	Steel	<input type="checkbox"/>	<input type="checkbox"/>	<input type="checkbox"/>	<input type="checkbox"/>	Timber	<input type="checkbox"/>	<input type="checkbox"/>	<input type="checkbox"/>	<input type="checkbox"/>	Masonry	<input type="checkbox"/>	<input type="checkbox"/>	<input type="checkbox"/>	<input type="checkbox"/>	Composite Steel-RC	<input type="checkbox"/>	<input type="checkbox"/>	<input type="checkbox"/>	<input type="checkbox"/>	Absent	<input type="checkbox"/>	<input type="checkbox"/>	<input type="checkbox"/>	<input type="checkbox"/>	Not identified	<input type="checkbox"/>	<input type="checkbox"/>	<input type="checkbox"/>	<input type="checkbox"/>	Other materials	<input type="checkbox"/>	<input type="checkbox"/>	<input type="checkbox"/>	<input type="checkbox"/>	Vertical structure	Absent	Seismic resistant system			Intermediate floor		Frame	Walls	Archs	Absent	<input type="checkbox"/>	<input type="checkbox"/>	<input type="checkbox"/>	<input type="checkbox"/>	Not identified	<input type="checkbox"/>	<input type="checkbox"/>	<input type="checkbox"/>	<input type="checkbox"/>	In plane deformable floor	<input type="checkbox"/>	<input type="checkbox"/>	<input type="checkbox"/>	<input type="checkbox"/>	In plane rigid floor	<input type="checkbox"/>	<input type="checkbox"/>	<input type="checkbox"/>	<input type="checkbox"/>	Materials	Transv. Dir.		Long. Dir.		Timber	Steel			Single diagonal	<input type="checkbox"/>	<input type="checkbox"/>	<input type="checkbox"/>	<input type="checkbox"/>	MRF	<input type="checkbox"/>	<input type="checkbox"/>	<input type="checkbox"/>	<input type="checkbox"/>	Concentric X braces	<input type="checkbox"/>	<input type="checkbox"/>	<input type="checkbox"/>	<input type="checkbox"/>	Concentric K braces	<input type="checkbox"/>	<input type="checkbox"/>	<input type="checkbox"/>	<input type="checkbox"/>	Concentric V braces	<input type="checkbox"/>	<input type="checkbox"/>	<input type="checkbox"/>	<input type="checkbox"/>	Eccentric braces	<input type="checkbox"/>	<input type="checkbox"/>	<input type="checkbox"/>	<input type="checkbox"/>	<p><b>Section D: Characterization of the structural members</b></p> <p><b>D1) Typology</b></p> <table border="1"> <tr> <td><input type="checkbox"/> Column</td> <td><input type="checkbox"/> Strut</td> <td><input type="checkbox"/> Massive timber</td> </tr> <tr> <td><input type="checkbox"/> Primary beam</td> <td><input type="checkbox"/> Diagonal</td> <td><input type="checkbox"/> Glulam timber</td> </tr> <tr> <td><input type="checkbox"/> Secondary beam</td> <td><input type="checkbox"/> King post</td> <td><input type="checkbox"/> CLT</td> </tr> <tr> <td><input type="checkbox"/> Brace</td> <td><input type="checkbox"/> Tie</td> <td><input type="checkbox"/> MDF</td> </tr> <tr> <td><input type="checkbox"/> Plank</td> <td><input type="checkbox"/> Other</td> <td><input type="checkbox"/> OSB</td> </tr> <tr> <td><input type="checkbox"/> Panel</td> <td></td> <td><input type="checkbox"/> LVL</td> </tr> <tr> <td><input type="checkbox"/> Other</td> <td></td> <td><input type="checkbox"/> Other</td> </tr> </table> <p><b>D2) Material</b></p> <p><b>D3) Timber specie</b></p> <p><input type="checkbox"/> Softwood <input type="checkbox"/> Hardwood <input type="checkbox"/> Not recognized</p> <p><b>D4) Year of construction</b></p> <table border="1"> <tr> <td><input type="checkbox"/> &lt; 1950</td> <td><input type="checkbox"/> 1972 - 75</td> <td><input type="checkbox"/> 1987 - 91</td> <td><input type="checkbox"/> 2002 - 08</td> <td><input type="checkbox"/> 2015 - 17</td> </tr> <tr> <td><input type="checkbox"/> 1950 - 81</td> <td><input type="checkbox"/> 1976 - 81</td> <td><input type="checkbox"/> 1992 - 96</td> <td><input type="checkbox"/> 2009 - 11</td> <td><input type="checkbox"/> 2018 - 20</td> </tr> <tr> <td><input type="checkbox"/> 1992 - 71</td> <td><input type="checkbox"/> 1982 - 86</td> <td><input type="checkbox"/> 1997 - 01</td> <td><input type="checkbox"/> 2012 - 14</td> <td><input type="checkbox"/> &gt; 2020</td> </tr> </table> <p><b>D5) Floor</b></p> <p><b>Above ground</b></p> <table border="1"> <tr><td><input type="checkbox"/> 1</td></tr> <tr><td><input type="checkbox"/> 2</td></tr> <tr><td><input type="checkbox"/> 3</td></tr> <tr><td><input type="checkbox"/> 4</td></tr> <tr><td><input type="checkbox"/> 5</td></tr> <tr><td><input type="checkbox"/> 6</td></tr> </table> <p><b>Underground</b></p> <table border="1"> <tr><td><input type="checkbox"/> 0</td></tr> <tr><td><input type="checkbox"/> 1</td></tr> <tr><td><input type="checkbox"/> 2</td></tr> <tr><td><input type="checkbox"/> 3</td></tr> </table> <p><b>D6) Hazard class (335-1)</b></p> <table border="1"> <tr> <td><input type="checkbox"/> 1</td> <td>Indoor, dry</td> <td>M.C. &lt; 20%</td> </tr> <tr> <td><input type="checkbox"/> 2</td> <td>Indoor or covered, not exposed to environmental agents</td> <td>M.C. occasionally &gt; 20%</td> </tr> <tr> <td><input type="checkbox"/> 3</td> <td>Outdoor, not in contact with the ground, exposed to environmental agents</td> <td>M.C. frequently &gt; 20%</td> </tr> <tr> <td><input type="checkbox"/> 4</td> <td>Outdoor, in contact with the ground and/or water</td> <td>M.C. permanently &gt; 20%</td> </tr> <tr> <td><input type="checkbox"/> 5</td> <td>Permanently and regularly immersed in salt water</td> <td>M.C. permanently &gt; 20%</td> </tr> </table> <p><b>D7) Average environmental temperature</b></p> <table border="1"> <tr> <td><input type="checkbox"/> &lt; 10°</td> <td><input type="checkbox"/> 10° - 20°</td> <td><input type="checkbox"/> 20° - 30°</td> <td><input type="checkbox"/> &gt; 30°</td> </tr> </table> <p><b>D8) Class of durability (EN 350-1)</b></p> <table border="1"> <tr> <td><input type="checkbox"/> 1 - Very durable</td> <td><input type="checkbox"/> 2 - Durable</td> <td><input type="checkbox"/> 3 - Moderately durable</td> <td><input type="checkbox"/> 4 - Slightly durable</td> <td><input type="checkbox"/> 5 - Not durable</td> </tr> </table>	<input type="checkbox"/> Column	<input type="checkbox"/> Strut	<input type="checkbox"/> Massive timber	<input type="checkbox"/> Primary beam	<input type="checkbox"/> Diagonal	<input type="checkbox"/> Glulam timber	<input type="checkbox"/> Secondary beam	<input type="checkbox"/> King post	<input type="checkbox"/> CLT	<input type="checkbox"/> Brace	<input type="checkbox"/> Tie	<input type="checkbox"/> MDF	<input type="checkbox"/> Plank	<input type="checkbox"/> Other	<input type="checkbox"/> OSB	<input type="checkbox"/> Panel		<input type="checkbox"/> LVL	<input type="checkbox"/> Other		<input type="checkbox"/> Other	<input type="checkbox"/> < 1950	<input type="checkbox"/> 1972 - 75	<input type="checkbox"/> 1987 - 91	<input type="checkbox"/> 2002 - 08	<input type="checkbox"/> 2015 - 17	<input type="checkbox"/> 1950 - 81	<input type="checkbox"/> 1976 - 81	<input type="checkbox"/> 1992 - 96	<input type="checkbox"/> 2009 - 11	<input type="checkbox"/> 2018 - 20	<input type="checkbox"/> 1992 - 71	<input type="checkbox"/> 1982 - 86	<input type="checkbox"/> 1997 - 01	<input type="checkbox"/> 2012 - 14	<input type="checkbox"/> > 2020	<input type="checkbox"/> 1	<input type="checkbox"/> 2	<input type="checkbox"/> 3	<input type="checkbox"/> 4	<input type="checkbox"/> 5	<input type="checkbox"/> 6	<input type="checkbox"/> 0	<input type="checkbox"/> 1	<input type="checkbox"/> 2	<input type="checkbox"/> 3	<input type="checkbox"/> 1	Indoor, dry	M.C. < 20%	<input type="checkbox"/> 2	Indoor or covered, not exposed to environmental agents	M.C. occasionally > 20%	<input type="checkbox"/> 3	Outdoor, not in contact with the ground, exposed to environmental agents	M.C. frequently > 20%	<input type="checkbox"/> 4	Outdoor, in contact with the ground and/or water	M.C. permanently > 20%	<input type="checkbox"/> 5	Permanently and regularly immersed in salt water	M.C. permanently > 20%	<input type="checkbox"/> < 10°	<input type="checkbox"/> 10° - 20°	<input type="checkbox"/> 20° - 30°	<input type="checkbox"/> > 30°	<input type="checkbox"/> 1 - Very durable	<input type="checkbox"/> 2 - Durable	<input type="checkbox"/> 3 - Moderately durable	<input type="checkbox"/> 4 - Slightly durable	<input type="checkbox"/> 5 - Not durable	<p><b>Section E: Decay effects identification</b></p> <p><b>E1) Colour</b></p> <table border="1"> <tr><td><input type="checkbox"/> Dark</td></tr> <tr><td><input type="checkbox"/> White - yellow</td></tr> <tr><td><input type="checkbox"/> Light blue</td></tr> <tr><td><input type="checkbox"/> No colour alteration</td></tr> <tr><td><input type="checkbox"/> Others</td></tr> </table> <p><b>E2) Aspect to the touch</b></p> <table border="1"> <tr><td><input type="checkbox"/> Dusty</td><td><input type="checkbox"/> Wet</td></tr> <tr><td><input type="checkbox"/> Fluffy</td><td><input type="checkbox"/> Soft</td></tr> <tr><td><input type="checkbox"/> Bulky</td><td><input type="checkbox"/> Others</td></tr> </table> <p><b>E3) Superficial aspect</b></p> <table border="1"> <tr><td><input type="checkbox"/> Presence of stripes</td></tr> <tr><td><input type="checkbox"/> Presence of cracks</td></tr> <tr><td><input type="checkbox"/> Presence of exfoliation</td></tr> <tr><td><input type="checkbox"/> Thin intact layer</td></tr> <tr><td><input type="checkbox"/> Others</td></tr> </table> <p><b>E4) Cracks</b></p> <table border="1"> <tr><td><input type="checkbox"/> Longitudinal cracks</td></tr> <tr><td><input type="checkbox"/> Transversal cracks</td></tr> <tr><td><input type="checkbox"/> Superficial cracks 1-3 mm</td></tr> <tr><td><input type="checkbox"/> Deep cracks &gt; 4 mm</td></tr> <tr><td><input type="checkbox"/> Others</td></tr> </table> <p><b>E5) Presence of holes</b></p> <table border="1"> <tr> <td><input type="checkbox"/> Circular shape</td> <td><input type="checkbox"/> Oval shape</td> </tr> <tr> <td>Holes diameter</td> <td><input type="checkbox"/> 1 - 2 mm</td> </tr> <tr> <td></td> <td><input type="checkbox"/> 3 - 5 mm</td> </tr> <tr> <td></td> <td><input type="checkbox"/> &gt; 5 mm</td> </tr> <tr> <td></td> <td><input type="checkbox"/> Others</td> </tr> </table> <p><b>E6) Presence of galleries</b></p> <table border="1"> <tr><td><input type="checkbox"/> Visible galleries</td></tr> <tr><td><input type="checkbox"/> Not visible galleries</td></tr> <tr><td>Shape of galleries</td></tr> <tr><td><input type="checkbox"/> Circular</td></tr> <tr><td><input type="checkbox"/> Oval</td></tr> <tr><td><input type="checkbox"/> Others</td></tr> </table> <p><b>E8) Extent of damage</b></p> <p><b>E8_a) Tools for diagnostic</b></p> <table border="1"> <tr> <td><input type="checkbox"/> Core extracting tool</td> <td><input type="checkbox"/> Resistance drilling tool</td> <td><input type="checkbox"/> Penetration tool</td> <td><input type="checkbox"/> Other</td> </tr> </table> <p><b>E8_b) Location</b></p> <table border="1"> <tr> <td><input type="checkbox"/> End zone</td> <td><input type="checkbox"/> Middle zone</td> <td><input checked="" type="checkbox"/> Whole member</td> </tr> </table> <p><b>E9) Other aspects</b></p> <table border="1"> <tr> <td><input type="checkbox"/> Presence of beetles</td> <td><input type="checkbox"/> Presence of timber residuals</td> <td><input type="checkbox"/> Presence of excrescent</td> </tr> <tr> <td><input type="checkbox"/> Presence of mold</td> <td><input type="checkbox"/> Mold small</td> <td><input type="checkbox"/> Crawling nose</td> </tr> </table> <p><b>E10) Presence of existing treatments</b></p> <table border="1"> <tr> <td><input type="checkbox"/> Not recognizable</td> <td><input type="checkbox"/> Superficial treatment</td> <td><input type="checkbox"/> Deep treatment</td> </tr> <tr><td><input type="checkbox"/> Other</td></tr> </table> <p><b>E11) Moisture content (M.C.)</b></p> <table border="1"> <tr> <td><input type="checkbox"/> M.C. &lt; 20%</td> <td><input type="checkbox"/> 20% &lt; M.C. &lt; 30%</td> <td><input type="checkbox"/> M.C. &gt; 30%</td> </tr> </table>	<input type="checkbox"/> Dark	<input type="checkbox"/> White - yellow	<input type="checkbox"/> Light blue	<input type="checkbox"/> No colour alteration	<input type="checkbox"/> Others	<input type="checkbox"/> Dusty	<input type="checkbox"/> Wet	<input type="checkbox"/> Fluffy	<input type="checkbox"/> Soft	<input type="checkbox"/> Bulky	<input type="checkbox"/> Others	<input type="checkbox"/> Presence of stripes	<input type="checkbox"/> Presence of cracks	<input type="checkbox"/> Presence of exfoliation	<input type="checkbox"/> Thin intact layer	<input type="checkbox"/> Others	<input type="checkbox"/> Longitudinal cracks	<input type="checkbox"/> Transversal cracks	<input type="checkbox"/> Superficial cracks 1-3 mm	<input type="checkbox"/> Deep cracks > 4 mm	<input type="checkbox"/> Others	<input type="checkbox"/> Circular shape	<input type="checkbox"/> Oval shape	Holes diameter	<input type="checkbox"/> 1 - 2 mm		<input type="checkbox"/> 3 - 5 mm		<input type="checkbox"/> > 5 mm		<input type="checkbox"/> Others	<input type="checkbox"/> Visible galleries	<input type="checkbox"/> Not visible galleries	Shape of galleries	<input type="checkbox"/> Circular	<input type="checkbox"/> Oval	<input type="checkbox"/> Others	<input type="checkbox"/> Core extracting tool	<input type="checkbox"/> Resistance drilling tool	<input type="checkbox"/> Penetration tool	<input type="checkbox"/> Other	<input type="checkbox"/> End zone	<input type="checkbox"/> Middle zone	<input checked="" type="checkbox"/> Whole member	<input type="checkbox"/> Presence of beetles	<input type="checkbox"/> Presence of timber residuals	<input type="checkbox"/> Presence of excrescent	<input type="checkbox"/> Presence of mold	<input type="checkbox"/> Mold small	<input type="checkbox"/> Crawling nose	<input type="checkbox"/> Not recognizable	<input type="checkbox"/> Superficial treatment	<input type="checkbox"/> Deep treatment	<input type="checkbox"/> Other	<input type="checkbox"/> M.C. < 20%	<input type="checkbox"/> 20% < M.C. < 30%	<input type="checkbox"/> M.C. > 30%
Materials	Vertical	Intermediate floors	Roof	Foundation																																																																																																																																																																																																																																																				
R.C.	<input type="checkbox"/>	<input type="checkbox"/>	<input type="checkbox"/>	<input type="checkbox"/>																																																																																																																																																																																																																																																				
Prefabricated R.C.	<input type="checkbox"/>	<input type="checkbox"/>	<input type="checkbox"/>	<input type="checkbox"/>																																																																																																																																																																																																																																																				
Steel	<input type="checkbox"/>	<input type="checkbox"/>	<input type="checkbox"/>	<input type="checkbox"/>																																																																																																																																																																																																																																																				
Timber	<input type="checkbox"/>	<input type="checkbox"/>	<input type="checkbox"/>	<input type="checkbox"/>																																																																																																																																																																																																																																																				
Masonry	<input type="checkbox"/>	<input type="checkbox"/>	<input type="checkbox"/>	<input type="checkbox"/>																																																																																																																																																																																																																																																				
Composite Steel-RC	<input type="checkbox"/>	<input type="checkbox"/>	<input type="checkbox"/>	<input type="checkbox"/>																																																																																																																																																																																																																																																				
Absent	<input type="checkbox"/>	<input type="checkbox"/>	<input type="checkbox"/>	<input type="checkbox"/>																																																																																																																																																																																																																																																				
Not identified	<input type="checkbox"/>	<input type="checkbox"/>	<input type="checkbox"/>	<input type="checkbox"/>																																																																																																																																																																																																																																																				
Other materials	<input type="checkbox"/>	<input type="checkbox"/>	<input type="checkbox"/>	<input type="checkbox"/>																																																																																																																																																																																																																																																				
Vertical structure	Absent	Seismic resistant system																																																																																																																																																																																																																																																						
Intermediate floor		Frame	Walls	Archs																																																																																																																																																																																																																																																				
Absent	<input type="checkbox"/>	<input type="checkbox"/>	<input type="checkbox"/>	<input type="checkbox"/>																																																																																																																																																																																																																																																				
Not identified	<input type="checkbox"/>	<input type="checkbox"/>	<input type="checkbox"/>	<input type="checkbox"/>																																																																																																																																																																																																																																																				
In plane deformable floor	<input type="checkbox"/>	<input type="checkbox"/>	<input type="checkbox"/>	<input type="checkbox"/>																																																																																																																																																																																																																																																				
In plane rigid floor	<input type="checkbox"/>	<input type="checkbox"/>	<input type="checkbox"/>	<input type="checkbox"/>																																																																																																																																																																																																																																																				
Materials	Transv. Dir.		Long. Dir.																																																																																																																																																																																																																																																					
	Timber	Steel																																																																																																																																																																																																																																																						
Single diagonal	<input type="checkbox"/>	<input type="checkbox"/>	<input type="checkbox"/>	<input type="checkbox"/>																																																																																																																																																																																																																																																				
MRF	<input type="checkbox"/>	<input type="checkbox"/>	<input type="checkbox"/>	<input type="checkbox"/>																																																																																																																																																																																																																																																				
Concentric X braces	<input type="checkbox"/>	<input type="checkbox"/>	<input type="checkbox"/>	<input type="checkbox"/>																																																																																																																																																																																																																																																				
Concentric K braces	<input type="checkbox"/>	<input type="checkbox"/>	<input type="checkbox"/>	<input type="checkbox"/>																																																																																																																																																																																																																																																				
Concentric V braces	<input type="checkbox"/>	<input type="checkbox"/>	<input type="checkbox"/>	<input type="checkbox"/>																																																																																																																																																																																																																																																				
Eccentric braces	<input type="checkbox"/>	<input type="checkbox"/>	<input type="checkbox"/>	<input type="checkbox"/>																																																																																																																																																																																																																																																				
<input type="checkbox"/> Column	<input type="checkbox"/> Strut	<input type="checkbox"/> Massive timber																																																																																																																																																																																																																																																						
<input type="checkbox"/> Primary beam	<input type="checkbox"/> Diagonal	<input type="checkbox"/> Glulam timber																																																																																																																																																																																																																																																						
<input type="checkbox"/> Secondary beam	<input type="checkbox"/> King post	<input type="checkbox"/> CLT																																																																																																																																																																																																																																																						
<input type="checkbox"/> Brace	<input type="checkbox"/> Tie	<input type="checkbox"/> MDF																																																																																																																																																																																																																																																						
<input type="checkbox"/> Plank	<input type="checkbox"/> Other	<input type="checkbox"/> OSB																																																																																																																																																																																																																																																						
<input type="checkbox"/> Panel		<input type="checkbox"/> LVL																																																																																																																																																																																																																																																						
<input type="checkbox"/> Other		<input type="checkbox"/> Other																																																																																																																																																																																																																																																						
<input type="checkbox"/> < 1950	<input type="checkbox"/> 1972 - 75	<input type="checkbox"/> 1987 - 91	<input type="checkbox"/> 2002 - 08	<input type="checkbox"/> 2015 - 17																																																																																																																																																																																																																																																				
<input type="checkbox"/> 1950 - 81	<input type="checkbox"/> 1976 - 81	<input type="checkbox"/> 1992 - 96	<input type="checkbox"/> 2009 - 11	<input type="checkbox"/> 2018 - 20																																																																																																																																																																																																																																																				
<input type="checkbox"/> 1992 - 71	<input type="checkbox"/> 1982 - 86	<input type="checkbox"/> 1997 - 01	<input type="checkbox"/> 2012 - 14	<input type="checkbox"/> > 2020																																																																																																																																																																																																																																																				
<input type="checkbox"/> 1																																																																																																																																																																																																																																																								
<input type="checkbox"/> 2																																																																																																																																																																																																																																																								
<input type="checkbox"/> 3																																																																																																																																																																																																																																																								
<input type="checkbox"/> 4																																																																																																																																																																																																																																																								
<input type="checkbox"/> 5																																																																																																																																																																																																																																																								
<input type="checkbox"/> 6																																																																																																																																																																																																																																																								
<input type="checkbox"/> 0																																																																																																																																																																																																																																																								
<input type="checkbox"/> 1																																																																																																																																																																																																																																																								
<input type="checkbox"/> 2																																																																																																																																																																																																																																																								
<input type="checkbox"/> 3																																																																																																																																																																																																																																																								
<input type="checkbox"/> 1	Indoor, dry	M.C. < 20%																																																																																																																																																																																																																																																						
<input type="checkbox"/> 2	Indoor or covered, not exposed to environmental agents	M.C. occasionally > 20%																																																																																																																																																																																																																																																						
<input type="checkbox"/> 3	Outdoor, not in contact with the ground, exposed to environmental agents	M.C. frequently > 20%																																																																																																																																																																																																																																																						
<input type="checkbox"/> 4	Outdoor, in contact with the ground and/or water	M.C. permanently > 20%																																																																																																																																																																																																																																																						
<input type="checkbox"/> 5	Permanently and regularly immersed in salt water	M.C. permanently > 20%																																																																																																																																																																																																																																																						
<input type="checkbox"/> < 10°	<input type="checkbox"/> 10° - 20°	<input type="checkbox"/> 20° - 30°	<input type="checkbox"/> > 30°																																																																																																																																																																																																																																																					
<input type="checkbox"/> 1 - Very durable	<input type="checkbox"/> 2 - Durable	<input type="checkbox"/> 3 - Moderately durable	<input type="checkbox"/> 4 - Slightly durable	<input type="checkbox"/> 5 - Not durable																																																																																																																																																																																																																																																				
<input type="checkbox"/> Dark																																																																																																																																																																																																																																																								
<input type="checkbox"/> White - yellow																																																																																																																																																																																																																																																								
<input type="checkbox"/> Light blue																																																																																																																																																																																																																																																								
<input type="checkbox"/> No colour alteration																																																																																																																																																																																																																																																								
<input type="checkbox"/> Others																																																																																																																																																																																																																																																								
<input type="checkbox"/> Dusty	<input type="checkbox"/> Wet																																																																																																																																																																																																																																																							
<input type="checkbox"/> Fluffy	<input type="checkbox"/> Soft																																																																																																																																																																																																																																																							
<input type="checkbox"/> Bulky	<input type="checkbox"/> Others																																																																																																																																																																																																																																																							
<input type="checkbox"/> Presence of stripes																																																																																																																																																																																																																																																								
<input type="checkbox"/> Presence of cracks																																																																																																																																																																																																																																																								
<input type="checkbox"/> Presence of exfoliation																																																																																																																																																																																																																																																								
<input type="checkbox"/> Thin intact layer																																																																																																																																																																																																																																																								
<input type="checkbox"/> Others																																																																																																																																																																																																																																																								
<input type="checkbox"/> Longitudinal cracks																																																																																																																																																																																																																																																								
<input type="checkbox"/> Transversal cracks																																																																																																																																																																																																																																																								
<input type="checkbox"/> Superficial cracks 1-3 mm																																																																																																																																																																																																																																																								
<input type="checkbox"/> Deep cracks > 4 mm																																																																																																																																																																																																																																																								
<input type="checkbox"/> Others																																																																																																																																																																																																																																																								
<input type="checkbox"/> Circular shape	<input type="checkbox"/> Oval shape																																																																																																																																																																																																																																																							
Holes diameter	<input type="checkbox"/> 1 - 2 mm																																																																																																																																																																																																																																																							
	<input type="checkbox"/> 3 - 5 mm																																																																																																																																																																																																																																																							
	<input type="checkbox"/> > 5 mm																																																																																																																																																																																																																																																							
	<input type="checkbox"/> Others																																																																																																																																																																																																																																																							
<input type="checkbox"/> Visible galleries																																																																																																																																																																																																																																																								
<input type="checkbox"/> Not visible galleries																																																																																																																																																																																																																																																								
Shape of galleries																																																																																																																																																																																																																																																								
<input type="checkbox"/> Circular																																																																																																																																																																																																																																																								
<input type="checkbox"/> Oval																																																																																																																																																																																																																																																								
<input type="checkbox"/> Others																																																																																																																																																																																																																																																								
<input type="checkbox"/> Core extracting tool	<input type="checkbox"/> Resistance drilling tool	<input type="checkbox"/> Penetration tool	<input type="checkbox"/> Other																																																																																																																																																																																																																																																					
<input type="checkbox"/> End zone	<input type="checkbox"/> Middle zone	<input checked="" type="checkbox"/> Whole member																																																																																																																																																																																																																																																						
<input type="checkbox"/> Presence of beetles	<input type="checkbox"/> Presence of timber residuals	<input type="checkbox"/> Presence of excrescent																																																																																																																																																																																																																																																						
<input type="checkbox"/> Presence of mold	<input type="checkbox"/> Mold small	<input type="checkbox"/> Crawling nose																																																																																																																																																																																																																																																						
<input type="checkbox"/> Not recognizable	<input type="checkbox"/> Superficial treatment	<input type="checkbox"/> Deep treatment																																																																																																																																																																																																																																																						
<input type="checkbox"/> Other																																																																																																																																																																																																																																																								
<input type="checkbox"/> M.C. < 20%	<input type="checkbox"/> 20% < M.C. < 30%	<input type="checkbox"/> M.C. > 30%																																																																																																																																																																																																																																																						

Figure 8: Main sections of the SHA-T survey form, applied to Palazzo Petrucci (Naples) (Faggiano et al., 2022)

The SHA-T survey form has been applied to a sample of simple existing timber structures located in different municipalities of the Southern Italy (Gioia Sannitica and Naples), representative of recurrent types of constructions, structural types and decay, in order to evaluate reliability and effectiveness (Fig. 9). Filling the form allowed to identify the degraded elements, the type of degradation and highlight the most vulnerable criteria that could influence the structural behavior of the system.

Table 2 - Outline of the SHA-T survey form.

Scope	Section	Description
	A	Identification of municipality and building
Building identification	B	Identification of the building constructive technology and typology
	C	Description of the building
	D	Characterization of the structural members
Timber decay detection	E	Decay effects identification
	F	Decay typology
	G	Possible interventions and treatments

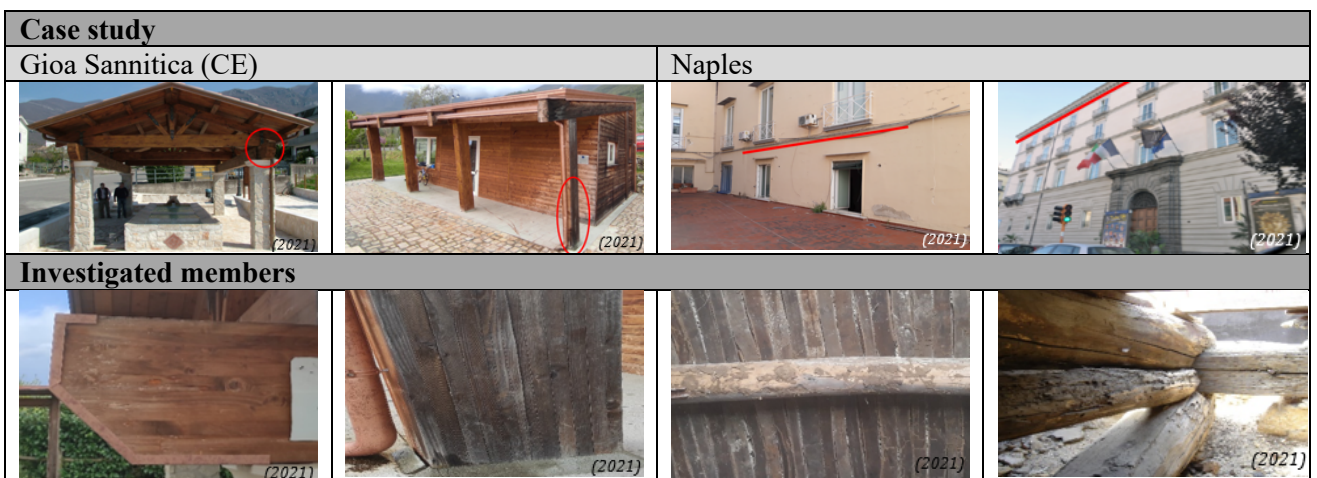


Figure 9: Case studies for the application of the SHA-T survey form (Marranzini et al., 2023)

The second survey form (Faggiano et al., 2025) has been conceived with a specific focus on timber trusses, in cooperation with the Italian IWC (Italian ICOMOS Wood Committee; ICOMOS Council of monuments and sites), whose mission is to promote the conservation, protection, safety and sustainable management of the wooden built heritage. The survey form is conceived not only as an operational tool

for the survey and diagnosis of timber trussed structures, but also for the development of a database for the inventory of the most common historic structural types and recurrent structural issues. The IWC form consists of the following 5 macro-sections, using a top-down approach: *building identification*; *building description*; *identification of the building components and structural units*; *survey*; *diagnosis* (Tab. 3).

Table 3 - Outline of the IWC survey form

Scope	Section	Description
Building analysis	1	Building identification
	2	Building description
	3	Identification of the building components and structural units
Typological and technological survey	4	Survey
	4.1	Survey of the structural unit
	4.2	Survey of the structural member
Assessment of the state of conservation	4.3	Survey of the structural nodes
	5	Diagnosis
	5.1	Diagnosis of the structural unit
	5.2	Diagnosis of the structural member

The building is assumed as an assembly of multiple Building Components (BC), such as intermediate floors, roof systems and walls. Each BC may include one or more Structural Units (SU), i.e. a roof component can consist of several trusses. In turn, each SU is composed of several Structural Members and Structural Nodes, i.e. a truss typically comprises members like struts, tie-beams, rafters, connected through nodes. The IWC survey form was applied to the timber roof of the Diplomatic Hall of the Royal Palace of Naples in order to assess the versatility, reliability and effectiveness, and then to validate it (Faggiano et al., 2025); Fig. 10).

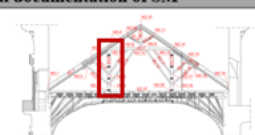


4.2. SURVEY OF THE STRUCTURAL MEMBERS (SM)					
Structural member (SM)	Queen post				
ID	SM.4				
Identification of the wood species			Type of woodworking		
Criteria	Data	Note	Criteria	Data	Note
Through macroscopic inspection	Chestnut (Castanea Sativa Mill.)		Unbraked / Rounded	YES	
Through microscopic inspection			Sawn finish	NO	
Existing documentation	Intervention of structural retrofit		Hewing finish	NO	
Age of the SM	1600-1700	reference: Mazzolani et al., 2009	Type of superficial treatment		
Geometry and dimension			Criteria	Data	Note
Criteria	Data	Note	Not visible	YES	
Type of cross section	Composed cross-section	The cross section consists of a main member with circular geometry and a pair of outer slices with rectangular geometry	Wood oil	NO	
Geometry of the member	Costant cross-section		Varnishing	NO	
Geometry of the cross-section	Circular		Painting	NO	
Average sizes of the cross-section [cm]	D=18		Carving decoration	NO	
Member length [m]	4,00		Wax	NO	
			Other	NO	
Graphical documentation of SM					
					
Structural section with evidence of the SM.4		View of the SM.4 in correspondence of the nodes SN.5, SN. 6		Frontal view of the SM.4	

Figure 10: Example of application of the IWC form to the Royal Palace of Naples (Faggiano et al., 2025)

### Mechanical characterization of existing timber structures through non destructive tests

In the structural health monitoring of timber structures, to identify structural vulnerabilities, degradation phenomena and to quantify the impact of degradation on structural performance, it is essential to achieve an adequate level of knowledge through the accurate estimation of mechanical properties. Non-destructive techniques (NDT) provide a viable alternative to destructive laboratory testing, by allowing the evaluation of physical and mechanical properties of timber elements through in-situ investigations without compromising member integrity, which has to be preserved specially in historic buildings. However, NDT reliability depends on the availability of robust correlations between NDT-derived

parameters and the physical and mechanical properties obtained from destructive tests (DT). In this regard, an experimental campaign was performed on a sample of 18 timber members, made of Chestnut (*Castanea sativa*, CS; 5 specimen) and Corsican Pine (*Pinus nigra* subsp. *laricio* (Poir.) Maire, PNL; 13 specimen), at the University of Calabria, in collaboration with the University of Florence, the National Research Council (CNR-IBE), the Soprintendenza Archeologia Belle Arti e Paesaggio of the Cosenza Province (Fig. 11; (Verre et al., 2023; Marranzini et al., 2025).

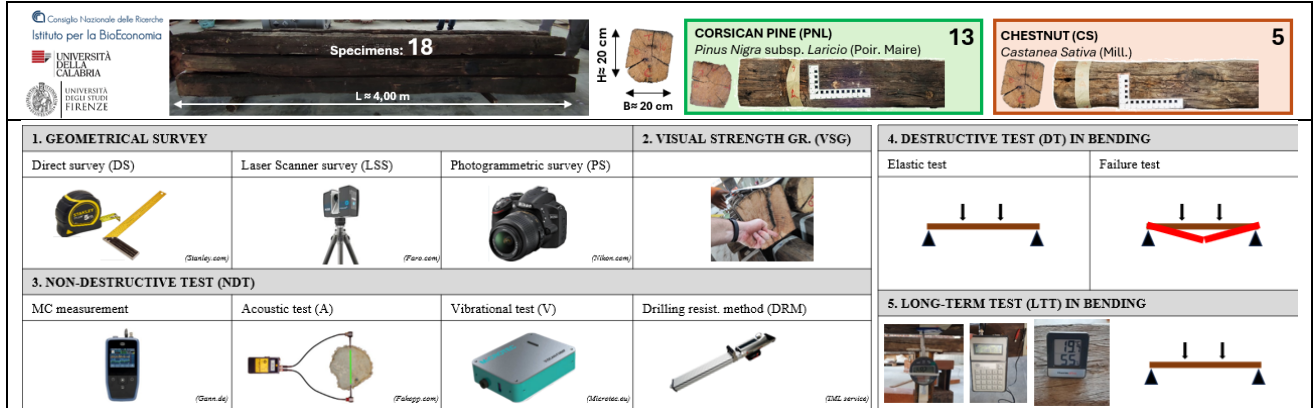


Figure 11: Specimen and Methods (Verre et al., 2023; Marranzini et al., 2025)

The following activities were carried out: geometrical survey by both Direct (DS) and indirect survey methods, such as Laser Scanner Survey (LSS) and Photogrammetric Survey (PS); Visual Strength Grading (VSG); Non Destructive Test (NDT), such as Acoustic (AT) and Vibrational Tests (VT), to evaluate the Dynamic Modulus of Elasticity (MOEdyn), Drilling Resistance Test (DRT) to evaluate the mean drilling resistance ( $R_m$ ), which has a good correlation with the material density; Destructive Test (DT) in bending, to evaluate local and global Moduli of Elasticity ( $E_{m,l}$ ,  $E_{m,g}$ ), bending resistance ( $f_m$ ) and modes of failure. Also the Moisture Content (MCCS=14.7%, MCPNL=17.2%) and the density ( $\rho_{CS}=539\text{kgm}^{-3}$ ,  $\rho_{PNL}=570\text{kgm}^{-3}$ ) of the specimen were measured. Details on the specimen survey, timber grading and experimental outputs can be found in Verre et al. (2023) and Marranzini et al. (2025).

With regard to the NDT-DT correlations, some of them are shown in Fig. 12. In particular it has been noticed that among the NDT correlations, strong relationships were found between drilling resistance measurements ( $R_m$ ) and Dynamic Modulus of Elasticity (MOEdyn), particularly using vibrational methods. DT correlations show very high linearity between bending strength ( $f_m$ ) and Global Modulus of Elasticity ( $E_{m,g}$ ) for both species. The most promising outcomes emerged from NDT-DT correlations: for PNL, high coefficients of determination ( $R^2$ ) were consistently observed between Dynamic Modulus of Elasticity (MOEdyn) and both bending strength ( $f_m$ ) and Global Modulus of Elasticity ( $E_{m,g}$ ), indicating the effectiveness of acoustic and vibrational methods in capturing mechanical behavior. Conversely, for CS, the presence of an outlier notably reduced correlation reliability, emphasizing the need for an extension of the sample and for potential outlier mitigation in future studies. In the end, the findings suggest that NDT methods, especially when correlated with reliable DT data, can serve as effective proxies for mechanical characterization in on site assessment of existing timber structures.

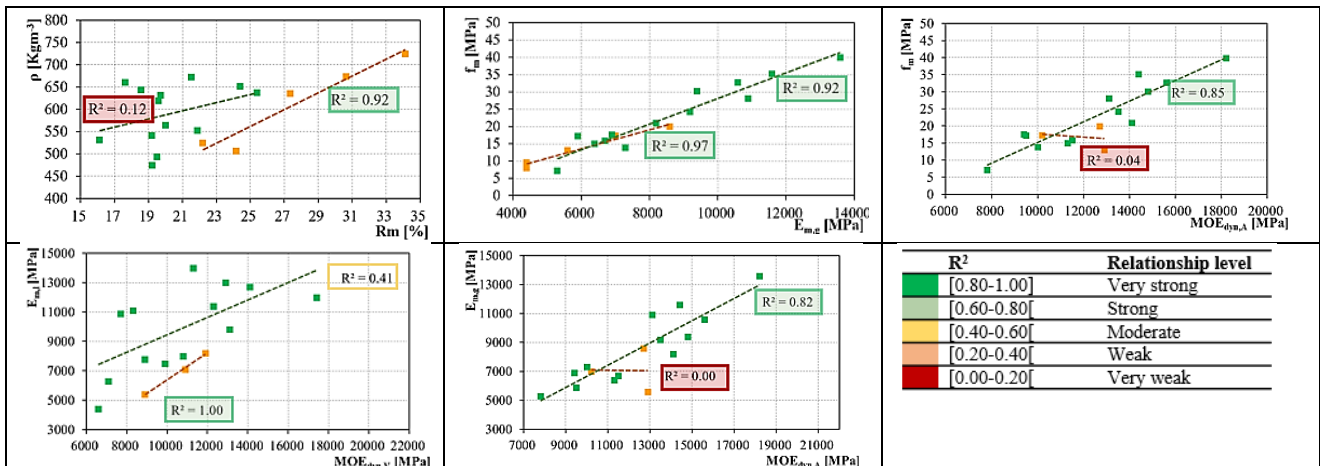


Figure 12: Some of the linear correlations analyzed (Marranzini et al., 2025)

### Conclusion:

In the framework of the structural vulnerability assessment of existing timber constructions, with particular reference to those exposed to seismic and volcanic risks, integrating aspects related to durability and material degradation, the two survey forms developed, the SHA-T and the IWC forms, results to be useful tools for guiding the structural health assessment of timber constructions and the identification of degradation phenomena, through a hierarchical analysis of components, structural units, members and nodes. The application of these tools to selected case studies demonstrated the effectiveness in supporting systematic data acquisition, also aimed at the inventory of timber structures, and the identification of structural and conservation-related issues. These are also useful for the identification of criteria for the definition of synthetic index aimed at the development of quick level methods for the structural vulnerability assessment. In addition, to achieve an adequate level of knowledge, the survey phase must be complemented by in-situ investigations aimed at estimating the mechanical properties of the timber members. To this aim, the potential of non-invasive Nondestructive techniques to be applied in situ, through the correlations between measured parameters and the actual mechanical properties of the material, has been highlighted. Future progress will focus on the application of the proposed tools to additional case studies, expanding the sample size, and on the refinement of methodologies for the assessment of timber structures vulnerability, including the state of conservation, for the validation of the proposed models and the development of a robust and reliable quick-level methods.

## 5. Infrastructure vulnerability under multi-hazard and climate change

---

Transportation infrastructure systems, particularly bridges, are exposed to multiple hazards and long-term degradation processes that may significantly affect their structural performance. This section focuses on the assessment of bridge vulnerability considering the combined effects of ageing, environmental deterioration, fire and seismic loading. A life-cycle approach is presented to evaluate the seismic vulnerability of reinforced concrete bridge piers under climate change, modelling chloride-induced corrosion and its influence on structural performance over time. In parallel, a multi-risk framework is proposed to assess bridge vulnerability accounting for the combined effects of seismic action, ageing and fire, including the development of hazard classification procedures and fragility analyses for different damage scenarios. In addition, an advanced numerical framework is developed to investigate the residual seismic capacity of bridge foundations affected by scour, highlighting the importance of soil–structure interaction and degraded foundation conditions in vulnerability assessment

### 5.1 Life-cycle seismic vulnerability of bridges under climate change (POLIMI, Fabio Biondini)

Infrastructure networks consist of a large number of critical assets, such as bridges and viaducts, which are subjected over time to the detrimental effects of aging and deterioration processes, such as chloride-induced corrosion. These adverse effects, further exacerbated by the long-term variations in environmental parameters due to climate change, may progressively compromise structural safety, seismic capacity, and vulnerability over time. In this context, a proper modeling of degradation processes capable of accounting for future climate conditions is essential for an accurate life-cycle seismic vulnerability assessment of aging bridges. In this contribution, a simulation-based approach incorporating cellular automata modeling of chloride-induced corrosion is developed and applied to the life-cycle seismic vulnerability assessment of bridges under climate change is proposed. The proposed approach is applied to a reinforced concrete bridge pier under corrosion and multiple climate scenarios. The results allow the quantification of the impact of climate change on chloride diffusion, corrosion damage evolution, and seismic performance over time.

#### 5.1.1 Life-cycle seismic performance of bridges

During their service life, structures and infrastructure systems are required to meet prescribed performance levels to ensure operability and safety under multiple hazards, including earthquakes. Aging and various degradation processes can progressively reduce structural and seismic capacity over time, so that the required performance levels may no longer be satisfied (Biondini & Frangopol, 2019). Bridges and viaducts are often considered the most vulnerable components of infrastructure networks, as they represent functional bottlenecks and are highly susceptible to extreme events and major natural hazards. In case of collapse or severe damage, the entire network may experience significant traffic disruption and adverse short- and long-term socioeconomic impacts on the region. Among the different deterioration mechanisms, chloride-induced corrosion in (RC) structures is particularly critical, especially for RC bridges, whose structural members are frequently exposed to chloride ingress from de-icing salts or marine environments. In this context, proper modeling of degradation phenomena is fundamental to accurately estimate the time-dependent structural and seismic performance and residual capacity of the system.

#### 5.1.2 Effects of Climate Change

Climate change associated with continued greenhouse gas emissions causes global warming, which, in turn, leads to exacerbate multiple and concomitant hazards, increasing both magnitude and frequency of

extreme events and accelerating aging and structural deterioration processes (Biondini et al., 2024). Future changes in temperature  $T$  and relative humidity  $RH$  may affect corrosion mechanisms, by anticipating the onset of corrosion and increasing corrosion rate  $i_{corr}$ , leading to a further reduction of life-cycle structural and seismic vulnerability. In order to account for non-stationary climatic condition in the life-cycle seismic vulnerability assessment of bridges, a simulation-based approach based on cellular automata is considered (Nava et al., 2026). This approach accounts for the increase of the diffusion coefficient  $D$  over time  $t$  with temperature and relative humidity. Moreover, the influence on corrosion propagation, which starts when chloride concentration at the level of reinforcement attains a critical threshold  $C_{cr}(t)$ , is also considered based on the variation of the environmental parameters. In particular, critical chloride threshold is affected by temperature. Moreover, corrosion rate increases with temperature and chloride concentration  $Cl$ , decreases due to the formation of corrosion products  $R_p$ , and is strongly influenced by relative humidity. The proposed approach, including the formulations of diffusion coefficient  $D(t, T, RH)$ , critical chloride threshold  $C_{cr}(t, T)$ , and corrosion rate  $i_{corr}(t, T, RH, Cl, R_p)$ , are reported in Nava et al. (2026).

### 5.1.3 Case Study

The proposed approach is applied to the life-cycle seismic vulnerability and reliability assessment of the RC two-column bridge pier shown in Figure 13a (see Nava et al. 2026 for more details). Each column bent has a two cellular cross-section  $5\text{ m} \times 2.5\text{ m}$ . The columns are connected at the top by a pier cap.

The life-cycle seismic performance of the bridge pier is investigated at structural level, considering both a nominal and a probabilistic approach, assuming the column bents exposed to chloride attack over the inner and outer surfaces with uniform chloride concentration. Corrosion damage is modeled considering the reduction in the mass of steel reinforcement, concrete strength, and steel ductility. The probabilistic analysis accounts for uncertainties in mechanical and environmental damage stressors and deterioration process.

The analysis timeframe ranges from the year 2015 to the year 2100 and future climate projections are derived from the CNRM-CM6-1-HR climate model. Three climate scenarios based on the SSP-RCPs for Singapore are considered: (1) very high baseline emission scenario (SSP5-8.5); (2) mitigation scenario (SSP1-2.6); and (3) historical scenario which is obtained by repeating the climate projections from 1970 to 1980.

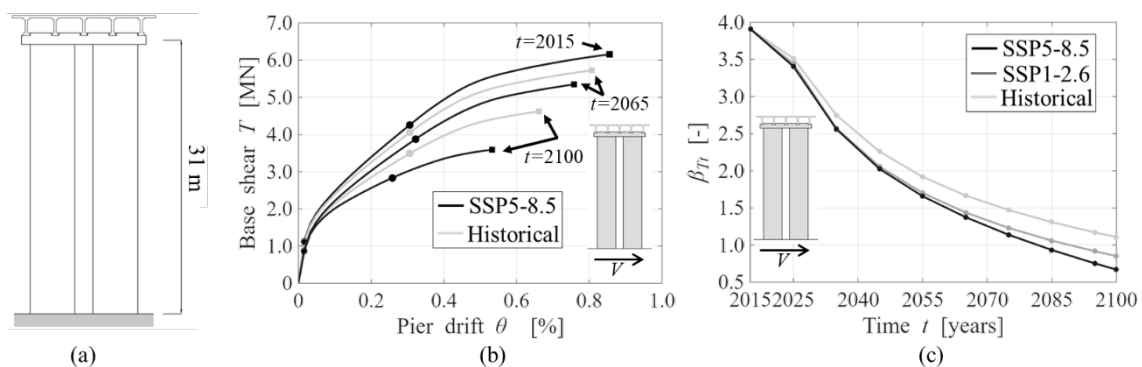


Figure 13. Life-cycle seismic reliability assessment of a RC bridge pier under historical and climate change scenarios: (a) Geometry; (b) Nominal base-shear versus pier drift; (c) Time-variant reliability index

Nonlinear pushover analysis is performed to investigate the seismic response of the RC bridge pier. The analyses have been carried out considering a load pattern consistent with the first modal vibration period. Figure 13b shows the nominal capacity curves in terms of total base shear  $V$  versus drift of pier  $\theta$  at the initial time, after fifty years and at the end of the century, for SSP5-8.5 and historical climate scenarios. Climate change involves a reduction in both ultimate base shear and pier drift.

Probabilistic analysis is carried out based on Monte Carlo simulation method. Life-cycle seismic reliability analysis is carried out at the system level considering as limit state the attainment of a target peak base

shear of  $T_t=3.4$  MN. The results are reported in Figure 13c in terms of time variant reliability index, associated to the attainment of the limit state function for the system response under the historical, SSP1-2.6, and SSP5-8.5 climate scenarios. The detrimental impact of climate change can be appreciated at the year 2100 by a more pronounced reliability index decay, quantified in a percentage reduction of approximately 23% for SSP1-2.6 and 40% for SSP5-8.5, with respect to historical climate. Additional results can be found in Nava et al. (2026).

### 5.1.4 Conclusions

This paper presented an approach to chloride diffusion simulation and damage corrosion modeling under climate change using non-stationary cellular automata for the life-cycle seismic vulnerability assessment of aging bridges. The approach is applied to the life-cycle seismic vulnerability assessment of an RC bridge pier. The results allow to quantify the detrimental impact of climate change on the time-variant seismic vulnerability and reliability of deteriorating bridges and highlight the need for a proper modelling of degradation processes considering the variation of the environmental parameters.

## 5.2 Assessment of multi-risk vulnerability for existing bridges (aging, fire, earthquake) (UNIPA, Piero Colajanni and Lidia La Mendola)

### 5.2.1 Bridges vulnerability to seismic action, aging and fire

In the multi-risk assessment of bridges, among the major sources of increased seismic vulnerability are the effects of ageing, with particular reference to reinforcement corrosion and concrete carbonation; a further source of risk, especially in areas characterised by the frequent passage of hydrocarbon tanks, such as those near refineries or along ring roads in urban areas with a high density of petrol stations, is the effect of fire triggered by seismic events or road accidents involving vehicles carrying highly flammable contents. While, in the literature, research addressing the seismic vulnerability of bridges subject to degradation phenomena due to ageing is well established (Gkournelos et al., 2021) and continuously evolving (Kuma et al., 2025), studies that also consider the effect of fire are rarer.

### 5.2.2 Methodology

Initially, a typological inventory was carried out on a set of 30 bridges within the Palermo metropolitan area, mostly located along the ring road and differing in structural typology, material, and type of load, and the most recurrent typologies and the structural features governing multi-hazard vulnerability were identified.

Then, a method for estimating fire hazards was reviewed and adapted (Granata et al., 2026) through an expert-based reweighting of the influencing factors to be assigned according to geometric characteristics, material properties, and design details, leading to a new classification into five hazard classes, compatible with the procedure followed by the Italian Guidelines on Existing Bridges. Subsequently, the seismic risk of the same bridges was also evaluated based on the methodology established by the Italian standard, in comparison with expedited methods accepted internationally, including the North American HAZUS model.

Subsequently, to assess the effects of aging, a simplified model was employed to estimate the reduction of the moment–axial force interaction domain of reinforced-concrete column cross-sections subjected to corrosion processes. The model accounts for cover spalling, buckling of longitudinal reinforcement, and loss of bond in tension bars, thereby allowing the estimation of the reduction in steel strength, reinforcement cross-sectional area, and the depth of the cracked zone within the concrete cover. With the aim of accounting for the effects of corrosion of transverse reinforcement, the flexure–shear interaction in corroded RC columns was modelled, taking into account basic cyclic strength and in-cycle strength degradation, stiffness degradation, and pinching.

Finally, the effects of possible fire load scenarios on reinforced concrete beams, columns, and walls were analysed. Specifically, fire development was numerically simulated on a specific type of road bridge using Computational Fluid Dynamics (CFD) (Colajanni et al., 2026), to benchmark the results against fire loads reported in the literature and design codes. The analysis considers variations in fire location and intensity, applying an advanced numerical framework to model fire effects and determine the resulting temperature distribution across the concrete elements.

Several case studies were analysed, including overpasses characterized by different pier typologies (structural schemes and cross-sectional shapes) and one case study involving a highway bridge. For each case, fragility curves were derived for three damage states, representing the uncertainty due to record-to-record variability, assuming as a representative parameter of the seismic intensity the ordinate of the elastic response spectrum corresponding to the fundamental period of vibration in the considered direction. Analyses were performed for intact piers (0), piers deteriorated by moderate fire (F1), corrosion and moderate fire (F1C1), piers exposed to large fire (worst-case scenarios among those considered) (F2), and piers exposed to fire after prior corrosion-induced deterioration, both with and without cover spalling (F2C1), for seismic action in the transversal (x) and longitudinal (y) directions, and for three locations of the fire damage in the column (A, B, C).

### 5.2.3 Results of parametric analyses and Case Study

The results showed that the increase in vulnerability detectable from the analysis of the framed piers (Fig. 1a) is always rather modest (Fig. 1b,c), with the exception of conditions that lead to the activation of brittle shear failure mechanisms, which can occur in the transverse direction of the seismic action in the presence of high corrosion of the stirrups. The former phenomenon is due to the limited reduction in stiffness caused by deterioration due to aging and fire, and to a substantially reduced dependence of the displacement required by the seismic action on the system's resistance, a parameter that is more significantly affected by damage.

As expected, the increase in vulnerability is slightly more pronounced for the severe damage limit state, where the increase in the displacement required as damage increases becomes more significant. Fig. 1c, which shows a detail of the fragility curves for the earthquake in the two directions, indicates that the frame pier exhibits greater vulnerability in the longitudinal direction, but the increase due to corrosion or fire damage is greater in the transverse direction.

By comparison of the responses of the different structural schemes considered, it emerges that rectangular and hollow square sections are significantly more vulnerable to the combined effects of aging and fire than solid circular sections. The increase in vulnerability is strongly influenced by the vibration period of the structural element, being more significant for stiffer members, which are also more prone to shear-type failure mechanisms under seismic loading.

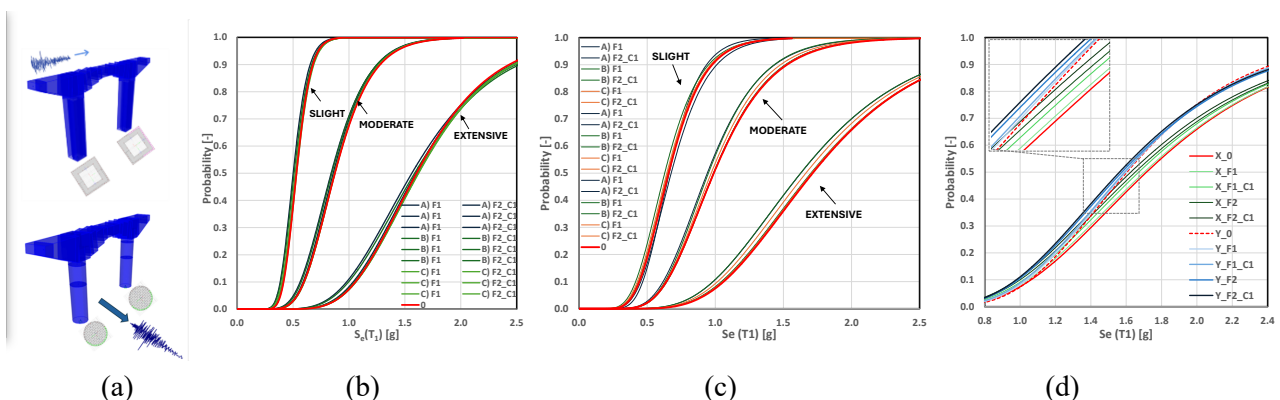


Figure 14. Fragility curves for RC bridge circular piers under seismic, aging and fire scenarios: (a) geometry; (b) longitudinal direction; (c) transversal direction (d)

Regarding the highway bridge case study featuring a framed scheme with a drop-in span, it was also observed that the higher vulnerability at the serviceability limit state (SLS) is mainly associated, in the absence of adequate restraint or bearing devices, with pounding and unseating phenomena in the

longitudinal direction. In particular, the localization of damage due to reinforcement corrosion and fire can significantly reduce the intensity of the seismic action capable of producing high probabilities of the bearings leaving their operating conditions.

## 5.3 Development and validation of innovative techniques for integrated rehabilitation – Residual seismic capacity of bridges across rivers (POLITO, Sebastiano Foti)

Foundation scour is a primary source of vulnerability for bridge infrastructure, exacerbated by the increasing frequency of extreme hydrological events due to climate change. As part of the RETURN project (Work Package 3.6), this report details the development and implementation of an advanced numerical framework for assessing the residual seismic capacity of scoured bridge foundations. The methodology incorporates an in-depth laboratory characterization of a reference granular material (SoFSI sand), calibration of the Pressure-Dependent-Multi-Yield (PDMY) constitutive model and implementation of a three-dimensional numerical model of a caisson-supported bridge pier. The findings show that scour significantly alters soil-structure interaction, resulting in reduced system stiffness, elongated natural periods, and increased permanent deformations.

### 5.2.1 Context and Problem Statement

Transportation networks are critical for modern society, yet bridges are frequently exposed to multiple natural hazards. Documentation indicates that foundation scour is responsible for over 50-60% of bridge failures worldwide. This often occurs without visible warning, as erosion takes place underwater. In a changing climate, increased flood exposure implies the need for a deeper understanding of how degraded foundation conditions interact with other hazards, such as earthquakes. Standard practice often relies on simplified seismic fragility curves or linear elastic soil models, which fail to capture the soil nonlinear, pressure-dependent behaviour or the complex geometry of local scour holes. This study addresses these issues by proposing an integrated framework that combines experimental soil data with advanced constitutive and numerical modelling.

### 5.2.2 Experimental Characterization of SoFSI Sand

The study used SoFSI sand, which is a natural, fine-grained silica sand. An extensive testing programme was conducted at the Politecnico di Torino to provide a physical basis for modelling. Triaxial tests (drained and undrained) were used to identify the critical state line. The cyclic and dynamic response was assessed through Resonant Column (RC) and Dynamic Simple Shear (DSS) tests to determine the small-strain shear modulus, stiffness degradation, and damping ratios. Figure 14A-C shows the typical results of the DSS test, conducted under displacement control at a specific confining level. The response is characterized by hysteresis loops with a decreasing slope and an increasing area with strain amplitude, together with accumulation of volumetric strains.

### 5.2.3 Constitutive Modeling and Numerical Implementation

The PDMY constitutive model was selected for its ability to simulate the behaviour of pressure-sensitive soil materials under static and cyclic loading. This elastic-plastic model uses Drucker-Prager conical yield surfaces and a non-associative flow rule to reproduce shear-induced volume changes. For this study, the parameters were calibrated using the laboratory data to ensure that the model accurately reflected the behaviour of the SoFSI sand. A 3D finite element model was then developed using OpenSees to simulate a reinforced concrete bridge pier supported by a rigid caisson foundation. To investigate the impact of foundation scour, three scenarios were modelled: No Scoured (NS), with a fully embedded foundation; General Scour (GS), with uniform soil removal; and Local Scour (LS), characterized by asymmetric 3D scour hole geometry derived from physical 1g modelling (Figure 14D).

### 5.2.4 Performance Analysis and Seismic Findings

First, the monotonic lateral response was assessed using pushover analysis. In general, foundation scour reduces both lateral and rotational stiffness. However, in the LS scenario, the system's resistance depends on whether the load was applied towards or away from the most scoured side. As for the dynamic response, free vibration analyses showed that foundation scour elongates the system's fundamental period compared to the unscoured state. Finally, seismic time-history analyses using real ground motion records demonstrated that, although scoured bridges might experience lower spectral accelerations (Figure 14E), this is offset by significantly higher displacement and rotation demands. The analyses also showed that peak acceleration-based demand measures alone are insufficient to describe the effects of scour, whereas cumulative and energy-based response indicators provide a more comprehensive representation of seismic performance under degraded foundation conditions.

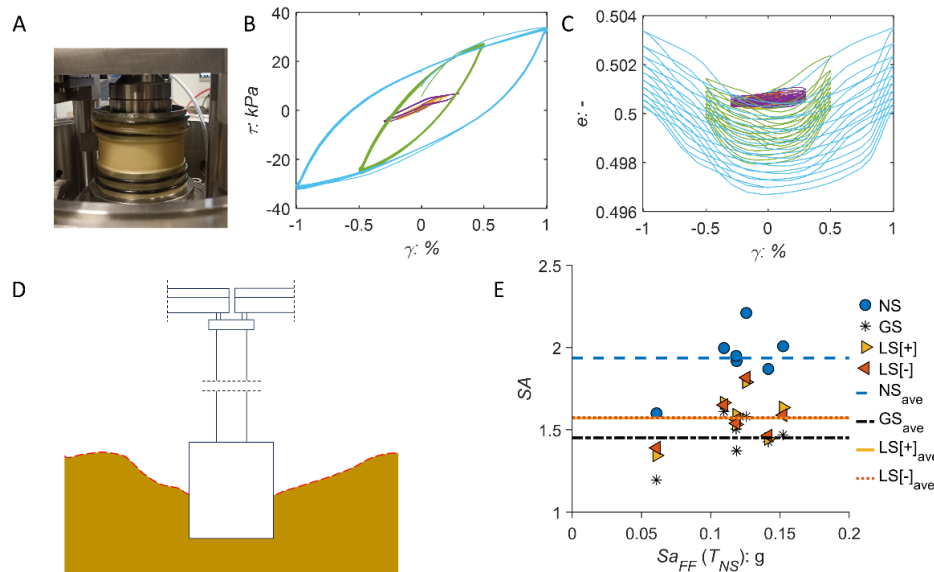


Figure 15: (A-C) DSS tests: A) specimen assembled in the DSS device; B-C) Results of DSS tests at a normal effective stress of 50 kPa, in terms of shear stress (B) and void ratio (C) vs shear strain loops. (D-E) Numerical model: D) Sketch of the numerical model, in the LS scenario, E) influence of the scour scenario on the deck spectral acceleration, for varying free-field spectral amplitude

### 5.2.5 Conclusions

The research developed an integrated framework that combines laboratory characterisation, constitutive modelling and numerical simulations in order to consider the influence of foundation scour on the dynamic behaviour of bridges, taking into account both the geometry and the soil response. The framework provides a physically consistent basis for assessing the seismic performance of bridge foundations under multiple hazard scenarios. The results highlight the reduced seismic demand on the superstructure and the increased displacement demands on the foundation in the presence of scour. Also, it was shown that cumulative energy-based indicators better capture the performance of scoured foundations than peak acceleration-based measures do. Ultimately, these results provide a consistent physical basis for risk-informed retrofitting and contribute to the RETURN project's goal of building resilient communities under a changing climate.

## 6. Vulnerability assessment methods for non-structural components and facilities

---

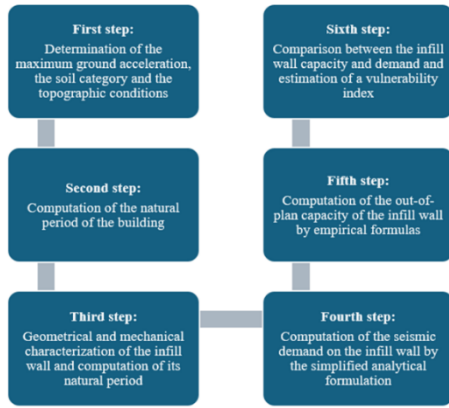
The seismic performance of buildings is influenced not only by the behaviour of primary structural systems but also by the vulnerability of secondary components and non-structural elements. This section presents methodologies aimed at improving vulnerability assessment at the component and facility scale. A simplified method is proposed for evaluating the out-of-plane vulnerability of masonry infill walls in reinforced concrete frames, combining analytical formulations with refined finite element modelling to estimate a vulnerability index and derive fragility curves for large-scale applications. In parallel, methodologies for seismic risk assessment of complex facilities are discussed, highlighting the importance of considering structural, non-structural and organizational aspects in vulnerability evaluation. An updated Rapid Visual Screening questionnaire is introduced to provide a rapid assessment of seismic risk in strategic facilities such as hospitals, integrating vulnerability indices and functionality indicators and supporting the prioritization of more detailed structural analyses.

### 6.1 Method to assess the frame-infill interaction in combined structural and energetic solutions (ENEA, Anna Marzo and Ivan Rosselli)

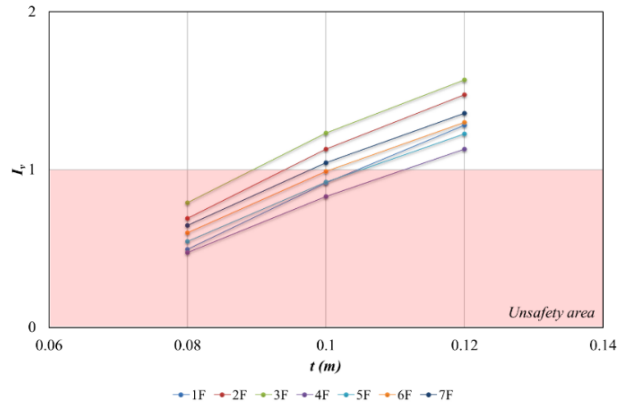
The vulnerability of infill walls, not designed to provide high thermal and mechanical performances, was the aim of this activity, which involved numerical analysis of common panels, adopted in non-recent buildings, mainly made of hollow clay-ceramic bricks and cement-lime mortar, cast in place with horizontal holes. The research began with an in-depth literature review, including both regulatory references and key research papers, meant to develop a simplified method to compute and compare seismic demand and out-of-plane capacity of infill walls, suitable for preliminary evaluations and large-scale applications. Subsequently, refined finite element models of bricks, mortar and walls were created to validate the simplified formulas taken from literature and finally obtain the fragility curves. To investigate the effects of the frame-infill interaction, three restraint conditions between the masonry panel and the surrounding frame were analysed: fully supported, separated by an upper gap, separated by lateral gaps.

#### 6.1.1 Infill panel FEM models and analyses

After having explored the main possibilities given in literature for calculating the out-of-plane demand and capacity of infill walls, through approaches alternative to finite element modelling, a simplified method for preliminary and large-scale evaluations of vulnerability has been developed. This method is organized into the six steps, summarised in Figure 15a, that lead to estimating a Vulnerability Index ( $I_v$ ), establishing that, if  $I_v < 1$ , the infill wall is likely to fail. Plotting it, for given seismicity level and panel mechanical and geometrical properties, as a function of the panel thickness ( $t$ ) and the building number of floors ( $F$ ) an unsafety area in the Cartesian plane can be highlighted. An explanatory sample is given in Figure 15b, in case of high seismicity, for panels made of mortar type M2.5 and bricks with characteristic compression strength 2MPa located at the top floor of the building and fully supported by the frame along the edges.



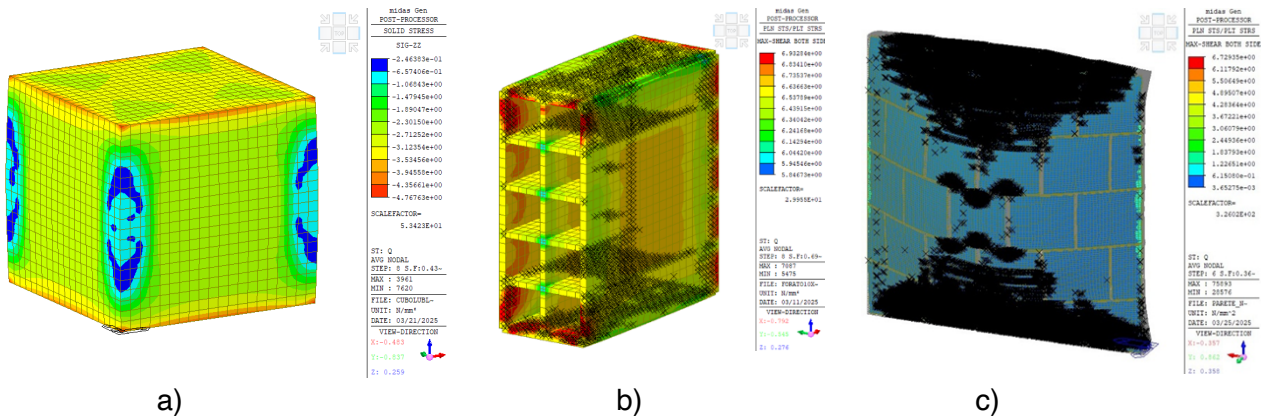
a)



b)

Figure 16: a) Method for preliminary estimation of infill wall vulnerability. b) Explanatory example

Then, a refined Finite Element (FE) analysis of a panel was used to validate the simplified formulas of the out-of-plane capacity proposed by Eurocode, which is based on Yield Line (YL) theory and assumes different strengths in vertical or horizontal directions, as well coefficients depending on the boundary conditions. Mortar type M2.5 and 10x25x25 cm bricks, with 5MPa compression strength in direction parallel to holes and >1.5 MPa orthogonally, have been added to model a masonry panel of 1.32x1.32 m with 1.2 cm of mortar joint thickness (Figure 16). Three numerical tests have been carried out by changing boundary conditions (restrained edges, gap at upper edge, gap at the side edges), repeating nonlinear analyses many times to reach the failure. The comparison between values of capacities obtained through FE and YL analyses suggested that, in the case of hollow clay bricks, the formulas deduced by YL theory overestimate the capacity if the compressive strength is used and should be corrected by a coefficient, which resulted reasonable to assume equal to 0.3.



a)

b)

c)

Figure 17: Numerical tests on: a) mortar specimen; b) hollow clay brick; c) fully restrained infill wall

The capacity thus assessed was used to finally obtain fragility curves for infill walls at a given site, assuming the boundary restraints of the infills as stochastic variables. The procedure was included in a computing script that automatically reads hazard data for a given site, and, based on mechanical and geometric characteristics of the infill, so as building height and panel elevation above ground, gives cumulative distribution function of the failure probability as a result, which is fitted by a lognormal distribution. The Figure 17 shows an explanatory example of the failure probability of a 3x3 m panel with  $t = 0.1$  m and the mechanical characteristics presented above, located at a height  $z = 11$  m on a 14-meter building. For the sake of the example, a site of coordinates Lat = 40.82706, Long = 14.13902 and hard soil were assumed.

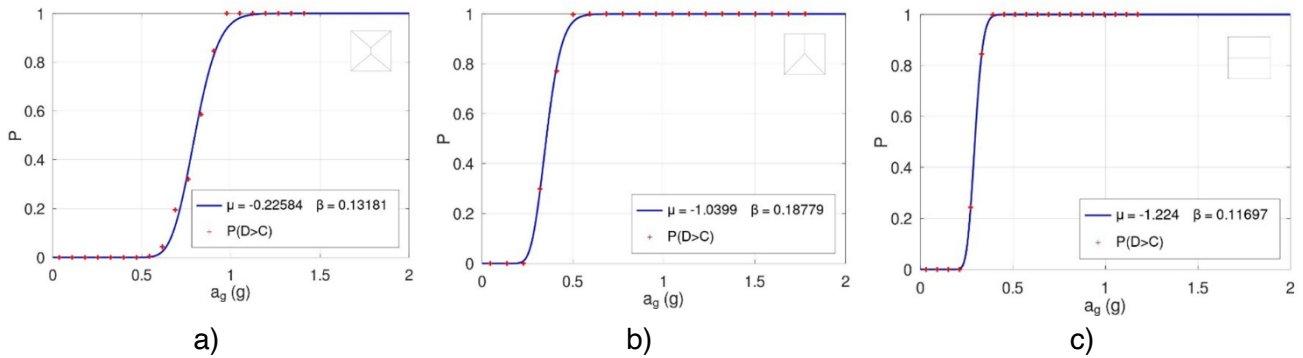


Figure 18: Example of failure probability curves in case of panels having: a) restrained edges; b) gap at upper edge; c) gap at side edges

### 6.1.2 Conclusions

A rational path to address the vulnerability of infill walls has been proposed. At first, given the site seismicity and the geometrical and mechanical properties of the panel, a simplified method was structured to establish the critical thickness depending on the number of floors of the reinforced concrete building. Then, after having derived the simplified formula of the out-of-plane capacity based on YL theory and corrected it to account for FE results, a computing script was developed to obtain territorial values of the failure probability of infills made of hollow clay bricks with horizontal holes. Some experimental investigations are needed for a complete validation of the method, which should be improved by introducing other stochastic variables that could be relevant for the results.

## 6.2 Seismic Risk Assessment Methodologies (UNINA, Gennaro Magliulo)

Earthquakes are among the deadliest natural hazards, and in Italy seismic risk is particularly high because hazard is medium–high, vulnerability is very high due to a fragile built environment, and exposure is high given population density and an exceptional cultural heritage. Since seismic risk depends on hazard, vulnerability, and exposure, assessing and upgrading existing buildings, especially strategic facilities like hospitals, is crucial, because post-earthquake functionality is often compromised less by structural failure than by damage to non-structural elements and equipment, which also account for most economic losses.

Building regulations, from historical provisions (e.g., Regio Decreto 16 November 1939) to current standards such as NTC 2018 (17 January 2018) with Circular No. 7 (21 January 2019) and Eurocode 8 (UNI EN 1998-1), define the safety criteria, analysis assumptions, design actions over the structure's nominal life, material properties, and verification procedures needed to assess and design earthquake-resistant structures, ensuring life safety, damage limitation, and the operability of strategic facilities.

Seismic risk assessment can be performed with qualitative methods that use descriptive ratings for a quick initial classification, or with quantitative methods that provide numerical indicators (e.g., probability of exceeding limit states, expected damage) based on theoretical models and advanced simulations. Rapid Visual Screening (RVS) offers a fast, low-cost, non-invasive preliminary estimate but is highly approximate, so it should be validated and complemented with detailed analyses such as non-linear static (pushover) and non-linear dynamic methods, which are more reliable but more time- and cost-intensive.

Seismic risk can be expressed as the combined effect of seismic hazard (HAZ), vulnerability (VULN), and exposure (EXP); however, to obtain a meaningful estimate, especially for complex facilities such as hospitals, vulnerability must include not only structural performance but also non-structural components (systems, equipment, architectural elements) and organizational aspects (emergency management, accessibility, procedures). Building on the Rapid Visual Screening (RVS) approach proposed by Perrone et al. (2015), an updated questionnaire was developed by extending and revising the original form: additional items were drawn from De Angelis and Pecce (2015), while some questions were removed or

reworded based on the UNINA research group's considerations. To facilitate interpretation, all questions were phrased negatively, so that an affirmative answer immediately indicates an increase in vulnerability. The final tool includes 109 questions, subdivided into 20 structural, 62 non-structural, and 27 organizational items, ensuring a more comprehensive representation of the factors that may compromise hospital safety and post-earthquake operability.

Each question is assigned to an Importance Level (LI), low, medium, or high, mapped to numerical values 1, 2, 3, respectively, derived from the unit vulnerability indices proposed by Perrone et al. (2015) and expert judgement. During inspection, the operator selects an expected Vulnerability Level (LV) (low/medium/high, again 1–3). A simplified rule addresses missing data and uncertainty: if a question is unanswered because it is not applicable, it is excluded from the evaluation; if it is unanswered but applicable, it is conservatively assigned high vulnerability. If an answer is provided with at least moderate uncertainty, the score is kept unchanged when LV is already high, otherwise the associated vulnerability contribution is increased by 50%. To quantify the impact of incomplete or uncertain information, the incompleteness index (iinc) (Terrizzi et al., 2018) was reformulated using the number of unanswered questions and uncertain answers, weighted by their importance; increasing iinc increases conservativeness and helps identify where additional data collection is most valuable.

Unit seismic vulnerability indices are computed as a function of LI and LV (with zero contribution when LV is low, and exponentially increasing values when LV is medium/high), and are normalized to obtain three Primary Vulnerability Indices: ISTR (structural), INSTR (non-structural), and IORG (organizational). A revised Functionality index (FUNC) is then introduced to better penalize poor non-structural performance even when the structure appears adequate:  $FUNC = (1 - 0.4 \cdot INSTR) \cdot (1 - ISTR)$ . Vulnerability is finally obtained by combining FUNC and IORG through a modified piecewise relationship that avoids discontinuities at low functionality. For hazard, the simplified zonation-based approach is refined by correlating HAZ to  $S_{ag}$  (where  $S = SS \cdot ST$  accounts for soil amplification and  $ag$  is selected based on nominal life and use class at SLV), and by limiting hazard's weight in the final score through a rescaled range 1–1.67; the proposed linear calibration is  $HAZ = 0.056 \cdot S_{ag} + 0.98$ . Exposure is classified into three levels (e.g., reference structures, ordinary structures, ambulatory facilities) with EXP values 1.25, 1.125, 1.00, respectively. The Seismic Risk Index (IRS) is then computed as  $IRS = VULN \cdot (HAZ/1.67) \cdot (EXP/1.25)$ , and classified as low (<0.33), medium (0.33–0.67), or high (>0.67), with the additional possibility of comparing IRS to an acceptable/target index to evaluate performance relative to the facility's role and required level of service after an earthquake.

Seismic analysis is essential in civil engineering because it predicts how a structure responds to earthquake-induced ground motion, quantifying internal forces and displacements to prevent collapse, reduce damage and downtime, and satisfy regulatory requirements (e.g., in Italy for new buildings and retrofits). Advanced methods can be read through three components: input (seismic action), object (structural model), and output (forces, displacements, performance). Regulations classify analyses by how seismic action is applied—static (equivalent lateral forces) or dynamic (accelerograms)—and by how behavior is modeled—linear (elastic) or non-linear (inelastic). This yields four main methods (NTC 2018 §7.3): Linear Static, Non-linear Static, Linear Dynamic, and Non-linear Dynamic.

A reliable assessment starts with the knowledge process, needed to build a representative model of geometry, stiffness, and masses. It typically includes: historical-critical analysis (construction period, modifications, past damage), survey (structural layout, dimensions, floors, non-structural elements, and detailing through checks such as reinforcement detection), and material characterization (in-situ tests for concrete/steel properties). These activities define a Level of Knowledge (LC1–LC3) and related confidence factors, which reduce mechanical parameters to account for uncertainty; when documentation is lacking, a simulated design may reconstruct likely reinforcement and detailing using historical standards and practices.

For existing RC buildings, non-linear modeling is often necessary to capture plasticity and degradation. Tools like OpenSees enable 3D FEM models for pushover and time-history analyses; common building-scale strategies use member-by-member models with lumped plasticity, where beams/columns are elastic in span and plastic hinges are concentrated at ends using zero-length elements and appropriate constitutive laws (e.g., IMK-type). Detailed analyses usually proceed from modal analysis (dynamic properties) to pushover (capacity curve, hinge development), and safety is governed by the most critical

mechanism, balancing ductile energy dissipation against potentially sudden brittle failures (often shear-related).

After detailed nonlinear seismic analyses, the building's displacement capacity at the Life Safety (SLV) and Collapse (SLC) limit states can be used to compute a structural seismic risk index as a demand–capacity ratio. Comparing this index with the RVS-based index often yields different results because pushover focuses on global structural response of load-bearing elements, while RVS also includes non-structural and organizational/functional components that strongly affect hospital operability. Additional discrepancies arise because the RVS procedure does not explicitly capture brittle failure mechanisms, suggesting the structural questionnaire should be revised to investigate these aspects. Overall, the findings support a multi-level approach: RVS is useful for rapid prioritization, but it should be calibrated against advanced models (e.g., OpenSees) and strengthened to better align screening outcomes with true structural capacity and failure modes.

The analysis shows that Italy's seismic risk is driven above all by the high vulnerability of an often pre-code building stock, and that for hospitals true resilience depends not only on structural safety but also on non-structural systems and organizational efficiency, so RVS is useful for rapid prioritization but must be validated and refined through detailed nonlinear (e.g., pushover/OpenSees) analyses, especially to capture brittle failure mechanisms, so that retrofit planning balances speed with scientific rigor and ensures post-earthquake operability.

## 5. Conclusions

---

The activities presented in this deliverable contribute to improving the assessment of vulnerability in the built environment under complex and evolving hazard scenarios. The studies highlight that vulnerability is not a static property of buildings and infrastructure systems but evolves over time as a consequence of cumulative damage, environmental degradation and interactions between different hazards.

The research presented in the first part of the report demonstrates the importance of modelling the temporal evolution of vulnerability. Frameworks for cumulative damage assessment, Markovian models for seismic damage accumulation and recovery, and reliability-based approaches for reinforced concrete structures provide tools for understanding how repeated seismic events and ageing processes influence structural performance. In addition, quick-level methodologies for the assessment of existing timber structures show how durability, degradation and in-situ characterization can be integrated into vulnerability evaluation.

The second part of the deliverable highlights the growing relevance of considering multi-hazard conditions and climate change in infrastructure assessment. Life-cycle analyses of bridges demonstrate that environmental deterioration processes such as chloride-induced corrosion may significantly affect seismic reliability over time, while the combined effects of aging and fire has significant influence on the vulnerability at serviceable limit state, and reduced one on the damage. Moreover, the analyses of scoured bridge foundations underline the importance of considering soil–structure interaction and degraded foundation conditions when evaluating seismic performance.

Finally, the studies on non-structural components and complex facilities emphasize that the overall seismic risk of buildings cannot be assessed solely through the behaviour of primary structural systems. The vulnerability of masonry infill walls and the role of non-structural and organizational components in facilities such as hospitals strongly influence building performance and post-earthquake functionality. Rapid visual screening methods, complemented by detailed nonlinear structural analyses, provide an effective framework for prioritizing interventions and improving risk management.

Overall, the results presented in this deliverable contribute to the development of integrated approaches for vulnerability assessment and support the broader objective of the RETURN project to enhance the resilience of communities facing evolving natural hazards and climate-related risks.

## 6. References

---

- Biondini, F., & Frangopol, D.M., (Eds.), 2019. Life-cycle design, assessment, and maintenance of structures and infrastructure systems. American Society of Civil Engineering (ASCE), Reston, VA, USA.
- Biondini, F., Lounis, Z., & Ghosn, M., (Eds.), 2024. Effects of climate change on life-cycle performance of structures and infrastructure systems: Safety, reliability, and risk. American Society of Civil Engineering (ASCE), Reston, VA, USA.
- Bruneau M, Chang SE, Eguchi RT, Lee GC, O'Rourke TD, Reinhorn AM, et al. A Framework to Quantitatively Assess and Enhance the Seismic Resilience of Communities. *Earthquake Spectra* 2003; 19(4): 733–752. DOI: 10.1193/1.1623497.
- Chioccarelli E, Iervolino I, Massimiliano Giorgio. Modelling seismic damage accumulation and recovery in aftershock sequences. In: Castanier B, Cepin M, Bigaud D, Berenguer C, editors. Proceedings of the 31st European Safety and Reliability Conference - ESREL 2021, Angers: Research Publishing, Singapore.; 2021.
- Colajanni, P., Granata, M. F., La Mendola, L., Stabile, M. (2024). Modelling of fire behavior of r.c. girders strengthened by external prestressing, *Procedia Structural Integrity, SMAR 2024, Proc. 7th International Conference on Smart Monitoring, Assessment and Rehabilitation of Civil Structures, Salerno (IT9, Settembre 2024)*.
- Costa R, Haukaas T, Chang SE. Agent-based model for post-earthquake housing recovery: <https://doi.org/10.1177/8755293020944175> 2020; 37(1): 46–72. DOI: 10.1177/8755293020944175.
- Cox DR, Miller HD. The theory of stochastic processes. Chapman and Hall; 1965. DOI: 10.1201/9780203719152/THEORY-STOCHASTIC-PROCESSES-COX-MILLER.
- De Angelis, A., Pecce, M., 2015. Seismic nonstructural vulnerability assessment in school buildings. *Nat Hazards* 79, 1333–1358. <https://doi.org/10.1007/s11069-015-1907-3>;
- De Iuliis, M., Miceli, E., Castaldo, P. (2024). Machine learning modelling of structural response for different seismic signal characteristics: a parametric analysis. *Applied Soft Computing Journal*, 164, 112026. <https://doi.org/10.1016/j.asoc.2024.112026>.
- De Iuliis, M., Miceli, E., Castaldo, P. (2025). An energy framework to control viscoelastic semi-active devices in plan-wise one-way asymmetric systems. *Structural Control and Health Monitoring*. 10.1155/stc/7091316.
- De Iuliis, M., Miceli, E., Castaldo, P. (2025). Information theory-guided machine learning to estimate seismic response of non-linear SDOF structures. *Engineering Structures*, 336, 120448. <https://doi.org/10.1016/j.engstruct.2025.120448>.
- Faggiano, B., Nicoletta, M., Iovane, G., Marranzini, D. (2022). A survey form for the structural health assessment of timber constructions. 6th Intern. Conf. Structural Health Assessment of Timber Constructions (SHATIS), 7-9 September 2022, Prague, Czech Republic.
- Gkournelos, P. D., Triantafyllou, T. C., & Bournas, D. A. (2021). Seismic upgrading of existing reinforced concrete buildings: A state-of-the-art review. *Engineering Structures*, 240, 112273.
- Granata, M. F., Cutrona, A., & Colajanni, P. (2026). Fire Importance Factor for Existing Urban Bridges According to Italian Guidelines Within a Fire–Seismic Multi-Risk Assessment. *Buildings*, 16(6), 1148.
- Granata, M. F., Grigoraş, Z. C., & Colajanni, P. (2026). Fire Load Effects on Concrete Bridges with External Post-Tensioning: Modeling and Analysis. *Buildings*, 16(2), 430.
- Iervolino I, Giorgio M, Polidoro B. Sequence-based probabilistic seismic hazard analysis. *Bulletin of the Seismological Society of America* 2014; 104(2): 1006–1012. DOI: 10.1785/0120130207.
- Iervolino I, Giorgio M, Chioccarelli E. Markovian modeling of seismic damage accumulation. *Earthquake Engineering & Structural Dynamics* 2016; 45(3): 441–461. DOI: 10.1002/eqe.2668.

- Iervolino I, Chioccarelli E, Suzuki A. Seismic damage accumulation in multiple mainshock–aftershock sequences. *Earthquake Engineering and Structural Dynamics* 2020; 49(10): 1007–1027. DOI: 10.1002/eqe.3275.
- Iervolino I, Giorgio M. Stochastic modeling of recovery from seismic shocks. 12th International Conference on Applications of Statistics and Probability in Civil Engineering, ICASP 2015, 2015.
- Iervolino I., Giorgio M., Chioccarelli E. Closed-form aftershock reliability of damage-cumulating elastic-perfectly-plastic systems. *Earthquake Engineering and Structural Dynamics* 2014; 43:613–625.
- Kumar, V., Singh, V., & Shekhar, S. (2025). State-dependent resilience of deteriorating bridges subjected to ground motion sequences. *Engineering Structures*, 336, 120402.
- Marranzini, D., Iovane, G., Cascini, L., Landolfo, R., Nicoletta, M., Faggiano, B. (2023). A methodology for the service life estimation of timber structures. *Life-Cycle of Structures and Infrastructure Systems (IALCCE)*. Open Access, Pages 3793 – 3799. Milan 2-6 July 2023. ISBN: 978-100332302-0. DOI: 10.1201/9781003323020-465.
- Marranzini, D., Iovane, G., Verre, S., Brunetti, M., Nocetti, M., Ruggieri, N., Togni, M., Ombres, L., Faggiano, B. (2025). Exploring correlations between non-destructive and destructive tests for the mechanical characterization of existing timber structures. *World Conference on Timber Engineering (WCTE)*. <https://doi.org/10.52202/080513-0414>.
- Marranzini, D., Verre, S., Iovane, G., Cauteruccio, G.F., Ruggieri, N., Brunetti, M., Nocetti, M., Togni, M., Ombres, L., Faggiano, B. (2025). Mechanical characterization of ancient timber members through destructive test in bending. 5th International Conference on Protection of Historical Constructions (PROHITECH). Naples, 26-28 March, 2025. [https://doi.org/10.1007/978-3-031-87316-4\\_20](https://doi.org/10.1007/978-3-031-87316-4_20)
- Miceli, E., Castaldo, P. (2024). Robustness improvements for 2D reinforced concrete moment resisting frames: parametric study by means of NLFE analyses. *Structural Concrete*, 25, 9–31.
- Miceli, E., De Iuliis, M., Castaldo, P. (2025). Robustness assessment of reinforced concrete structures for different failure scenarios. *Structural Concrete*. 10.1002/suco.70156.
- Miceli, E., Ferrara, S., Castaldo, P. (2024). Confinement effects within the seismic design of reinforced concrete frames: a reliability assessment and comparison. *Engineering Structures*, 313, 118248. <https://doi.org/10.1016/j.engstruct.2024.118248>.
- Miceli, E., Gino, D., Castaldo, P. (2025). Reliability assessment of robustness for reinforced concrete moment resisting frames. *Developments in the Built Environment*, 21, 100639. <https://doi.org/10.1016/j.dibe.2025.100639>.
- Miceli, E., Giordano, L., Castaldo, P. (2023). Probabilistic Evaluation of the Robustness of a Reinforced Concrete Frame Designed in a Seismic Area, *fib Young Italy 2023 – 3rd Symposium on Concrete and Concrete Structures*.
- Nava, G.V., D'Iorio, A., & Biondini, F., 2026. Nonstationary cellular automata for life-cycle assessment of concrete bridges under corrosion and climate change. *Structure and Infrastructure Engineering* (In press).
- Orlacchio M., Chioccarelli E., Iervolino I. State-dependent fragility functions for Italian building classes. *Soil Dynamics and Earthquake Engineering* 2024; 182 (2024) 108685.
- Perrone, D., Aiello, M.A., Pecce, M., Rossi, F., 2013. Rapid visual screening per strutture ospedaliere in cemento armato. *Proceeding in Anididis, L'ingegneria sismica in Italia*, Padova, Italia. Paper n. K11;
- Perrone, D., Aiello, M.A., Pecce, M., Rossi, F., 2015. Rapid visual screening for seismic evaluation of RC hospital buildings. *Structures* 3, 57–70. <https://doi.org/10.1016/j.istruc.2015.03.002>;
- Sberna, A.P., Deb, A., Di Trapani, F., Conte, J.P. (2025). Reliability-based seismic retrofitting design methodology for non-ductile reinforced concrete frame structures. *Probabilistic Engineering Mechanics*, 82, 103818.

- Terrizzi, A. R., Leone, M., Perrone, D., Uva, G., & Aiello, M. A. (2018). Valutazione del rischio sismico di edifici scolastici in calcestruzzo armato mediante una Scheda di Rapid Visual Screening Seismic risk evaluation of reinforced concrete school buildings through a Rapid Visual Screening Methodology. *Progettazione Sismica*, 10(2). <https://doi.org/10.7414/PS.10.2.35-48>
- Turchetti, F., Tubaldi, E., Patelli, E., Castaldo, P., Málaga-Chuquitaype, C. (2023). Damage modelling of a bridge pier subjected to multiple earthquakes: a comparative study. *Bulletin of Earthquake Engineering*, 21, 4541–4564. <https://doi.org/10.1007/s10518-023-01678-y>.
- UNI EN 1998-1:2005, Eurocodice 8. Progettazione delle strutture per la resistenza sismica. Parte 1: Regole generali, azioni sulle strutture e regole per gli edifici, UNI, 2005.
- Verre, S., Cauteruccio, G.F., Fortunato, G., Zappani, A.A., Ombres, L., Brunetti, M., Nocetti, M., Ruggieri, N., Togni, M., Marranzini, D., Iovane, G., Faggiano, B. (2023). Assessment of mechanical properties for ancient timber through visual and ND methods. *Life-Cycle of Structures and Infrastructure Systems (IALCCE)*. Open Access, Pages 3920- – 3926. Milan 2-6 July 2023. ISBN: 978-100332302-0. DOI: 10.1201/9781003323020-481.
- Yeo GL, Cornell CA. A probabilistic framework for quantification of aftershock ground-motion hazard in California: Methodology and parametric study. *Earthquake Engineering and Structural Dynamics* 2009; 38(1): 45–60. DOI: 10.1002/eqe.840.
- Zuccaro, G., Dolce, M., De Gregorio, D., Speranza, E. and Moroni, C. (2015). La scheda CARTIS per la caratterizzazione tipologico-strutturale dei comparti urbani costituiti da edifici ordinari. Valutazione dell'esposizione in analisi di rischio sismico. 34th National conference GNGTS (Gruppo Nazionale di Geofisica della Terra Solida). (In Italian).